学位申請論文

福岡　浩

Variation of the Friction Angle of Granular Materials in the High-Speed High-Stress Ring Shear Apparatus

— Influence of Re-orientation, Alignment and Crushing of Grains during Shear —

By Hiroshi FUKUOKA

Abstract

Using a newly developed high-speed high-stress ring shear apparatus, two series of ring shear tests on glass beads, sands, and clays were carried out under dry condition with no pore water pressure; first were the tests to change normal stress continuously during constant speed shearing. Second were the tests to give long shear displacement under a constant normal stress in a continuous test. Both of the test results showed variation of the friction angle during shear and it seemed to be related to grain crushing, re-orientation and alignment of grains. A careful examination of the grain size distribution, the sample height as well as the shear resistance during shear revealed; 1) grain crushing during shear causes generation of finer grains and it contributes to the increase of the friction angle during shear; 2) re-orientation of slender or platy grains parallel to the shear plane and alignment of grains along the shear direction causes decrease of friction angle during shear.

1. INTRODUCTION

In mitigating landslide disasters, prediction of the travel distance of landslides is important. However, it is a hard task since some landslides have traveled unexpectedly long distances. For example, in Japan, the Ontake landslide in 1984 (**Photo. 1**) traveled 12km, killing 15 people[1]. In China, the Sale landslide in 1983 traveled about 1 km and killed more than two hundred people[2]. In Canada, the Frank landslide in 1903 spread over an area of 2.7 km^2 and buried a town[3]. These landslides had low coefficients of friction in comparison with the usual values of internal friction angle of soils and rocks of about 30~40 degrees. Up to now, many researchers have tried to explain the mechanism of low coefficient of friction in the long-runout landslides such as those examples.

Scheidegger[4] defined the average coefficient of friction of a landslide as the ratio of total fall height to total travel distance, namely H/L (**Fig. 1**). He showed the relationship between the volumes of large landslides and their average coefficients of friction f by a diagram as **Fig. 1**. In this figure, the average coefficient of friction becomes smaller in larger landslides. He stated that the decrease of the average coefficient of friction became evident when the mass volume was larger than $10^4 m^3$, and he also reported that the average coefficient of friction remained constant and coincided with the tangent of the internal friction angle of the sliding material when the mass volume was smaller than $10^4 m^3$. In order to explain the decrease of the average coefficient of friction in larger landslides, several theories have been proposed: high rate of shearing by Hsü[5], and Davies[6]; acoustic fluidization by Melosh[7]; frictional heat by Habib[8], and Voight and Faust[9]; and undrained loading by Sassa[10], and Sassa et al.[11].

Exact and direct approach to the travel distance of landslides is the measurement of the coefficient of friction (the friction angle) during high-speed shearing. In order to investigate the friction angle during high-speed shearing, the ring shear test is the most appropriate method because it has no limit for shear displacement. Major prior researches

by the ring shear test are listed in Table 1.

Novosad (1964)

Novosad[12] developed a ring shear apparatus to measure the friction angle during shear of glass beads and sands, under low normal stresses up to 0.0247kgf/cm^2 He reported the friction angle during shear of 17.0° ~ 19.0° for glass beads, of 29.5° ~ 34.5° for sands, and observed no rate effect on the friction angle during shear for shear speeds between 0.48 and 47.5cm/sec.

Scarlett and Todd (1969)

Scarlett and Todd[13] developed a ring shear apparatus to measure the critical porosity at which the granular assembly starts to fluidize. The maximum normal stress was 0.065kgf/cm^2 and the maximum shear speed was 32.4cm/sec. The measured friction angle during shear was 25.7° ~ 34.2° for three sands of different diameters. No effect of shear speed or normal stress on the friction angle was observed.

Bridgwater (1972)

Bridgwater[14] developed a ring shear apparatus for low normal stress up to 0.255kgf/cm^2 and high shear speed up to 192cm/sec. He carried out tests on 2mm glass beads, and celon, polypropylene, polyethylene and polyester chips and measured the friction angle during shear and the rate effect and normal stress effect on shear resistance. The results indicated that the friction angle during shear of the glass beads under the normal stress up to 0.06kgf/cm^2 was 19.4° when the shear speed was 18cm/sec, and 20.8° when the shear speed was 186cm/sec.

The friction angle during shear of polyester chips and two kinds of polyethylene chips under normal stress up to about 0.05kgf/cm^2 varies $-1.0°, +1.2°$ and $+2.1°$, respectively, in two shear speeds of 18cm/sec and 190cm/sec. However, almost no rate effect was observed on the Celon chips in the same test condition.

He concluded that the friction angle during shear of granular materials depends on

shear speed and explained it by absorption of stress fluctuation as the molecular vibration energy of the material without giving any quantitative consideration.

Hungr and Morgenstern (1984)

Hungr and Morgenstern[15] developed a high-speed ring shear apparatus to study the high mobility of rock avalanches and measured the friction angle during shear of granular materials and examined the rate effect. The normal stress of their tests were up to 2.0kgf/cm^2 and shear speed was 98cm/sec, 16cm/sec (by motor) or lower than 0.1cm/sec (by hand). Samples were the Ottawa sands, sand and rock flour mixtures, and polystyrene beads. Results of the tests showed no remarkable rate effect. They concluded that the tested materials showed complete frictional characteristics, (namely the shear stress is in proportion to the normal stress) and the friction angle during shear was independent of shear speed over the range of conditions of the tests they made.

Sassa et al. (1984)

Sassa et al.[16] developed a low-stress high-speed ring shear apparatus and examined the friction angle during shear of 0.2mm glass beads, 1mm glass beads, the Toyoura standard sands, the Uji river sands, and the torrent deposits of the Denjo river on which the Ontake landslide traveled. The test condition was the normal stress up to 0.4kgf/cm^2 and shear speed of 0.01cm/sec $\sim$ 90cm/sec. Results of the tests showed no variation of friction angle during shear for the all samples over the range of the conditions.

Vibert et al. (1989)

Fukuoka et al. (1990)

Sassa et al.[17] developed a high-speed high-stress ring shear apparatus to investigate the friction angle during high-speed shearing. The available range of the conditions of the apparatus is 0.1 $\sim$ 3.8kgf/cm^2 of the normal stress and 0.01 $\sim$ 100cm/sec of the shear speed. Vibert et al.[18] Fukuoka et al.[19] carried out ring shear tests on 1mm glass beads and the torrent deposits of the Denjo river, and the Jizukiyama landslide soils. The results

are as follows;

1. Results on the 1mm glass beads showed no variation of the friction angle during shear for the shear speeds of 0.01, 0.1, 1, and 10cm/sec under normal stress up to 3.8kgf/cm^2. However, the friction angle during shear decreased by 2° at 100cm/sec.

2. Results of the ring shear tests on the torrent deposits of the Denjo river showed no variation in the friction angle for the shear speed of 0.01, 0.1, 1, and 10cm/sec under the normal stress up to 3.5kgf/cm^2. However, the friction angle during shear under the normal stress up to 1.7kgf/cm^2 at 100cm/sec increased by 1.5°, at which the motor stopped because of the upper limit of torque (**Fig. 2**).

3. Results of the ring shear tests on the Jizukiyama landslide soils showed variations of the friction angle; the conditions of the tests were normal stress up to 3.8kgf/cm^2, and the degree of saturation of the sample 20.8% ~ 26.1%. The friction angle of the soils was 32.8° for 0.01cm/sec, 35.0° for 0.1cm/sec, and 36.5° for 1.0 and 10cm/sec, the difference between the largest and smallest friction angles being 3.7° (**Fig. 3**).

4. Finely ground, powder-like soils were found on the shear plane after the tests. It implied that grain crushing had occurred at the shear plane. Grain crushing seemed to have some influence on the variation of the friction angle during shear.

Aim and Significance of This Study

Various theories to explain the low average coefficients of friction of landslides have been proposed. However, the arguments are diverse. The reason for the diverse opinions is that direct measurement of the coefficient of friction of real landslides in high speed motion is almost impossible, and also there have been few attempts to measure the friction angle during high-speed shearing under high normal stress. Therefore, it is very important to offer fundamental and reliable data of the friction angle of soils in high speed and high stress conditions using the High-Speed High-Stress Ring Shear Apparatus.

Until today, Hungr and Morgenstern[15] and Fukuoka et al.[19] have obtained some results on the measurement of the coefficient of friction during high-speed, high-stress shearing. However, the results of the rate effect on the coefficient of friction by the two groups did not coincide with each other; Hungr and Morgenstern[15] reported that there was no rate effect, while the results by Fukuoka et al.[19] showed some rate effects as shown in **Fig. 2 and 3**. However, the results by Fukuoka et al. showed both of positive and negative rate effects, depending on the kind of samples, and also the mechanism of variation of the coefficient of friction was not clarified. Greater variety of samples under different experimental conditions is desired to be tested.

Shear resistance during high-speed shearing may be understood to be the sum of two components; 1) shear resistance caused by grains without pore water, 2) variation of shear resistance affected by pore water (positive and negative pore pressure, and viscosity). In a ring shear apparatus, it is difficult to keep samples in undrained condition, and it is also difficult to measure pore pressure generated in the samples. In contrast, it is easy to maintain samples in a drained condition by using dry samples. To exclude uncertain factors, all tests in this study are done in the drained condition by using air-dried samples. This study was focused on the variation of the friction angle of grains during long and high-speed shearing without pore water.

In order to examine the friction angle during shear from plural aspects, two series of tests were carried out; A) the tests to change normal stress continuously during constant speed shearing, B) the tests to give long shear displacement under a constant normal stress.

The test results are presented in section 3 and the interpretation by the author on the mechanism of variation of the friction angle during shear is presented in section 4.

2. TEST APPARATUS AND PROCEDURE

2.1. Structure of the High-Stress High-Speed Ring Shear Apparatus

Fig. 4 is a schematic diagram of a High-Speed High-Stress Ring Shear Apparatus[17]. **Fig. 5** shows a cross section of the annular sample box. **Photo. 2** is the front view of the apparatus. The outside wall is made of transparent acrylic resin, retained by a metal frame so that the sample can be observed during test. Section of the sample box is 6cm wide and 6~8cm high. The loading plate can be moved vertically, so only the height of the sample can be changed. The sample box is separated horizontally at about midheight. The lower part of the sample box is rotated by a servo-controlled motor to shear the sample. Six porous metals with needles are fixed on the base and the ceiling (the loading plate) of the sample box for drainage and for preventing slippage of samples. After the start a shear test, a horizontal shear plane or shear zone is formed between the upper and the lower part of the sample box. There are rubber annular edges (as shown in **Fig. 5**) at the inside and outside gaps between the upper and the lower part of the sample box glued to the upper parts of the sample box to seal the gap, which is to prevent leakage of material from the sample box. A electric servo-controlled motor (connected to pulley A in **Fig. 4**) can rotate the lower part of the sample box at a constant speed. Available shear speed ranges between 0.001 cm/sec and 150 cm/sec with the use of four different gears in the gear box.

Normal stress is applied to the sample by an air compressor. The compressed air is supplied into six air-pistons through a servo-controlled air regulator. Six air-pistons push down the loading plate (ceiling of the sample box) and the normal stress is loaded on the sample. The maximum normal stress is 3.8kgf/cm^2

The gap distance between the upper and the lower part of the sample box should be strictly kept constant throughout the test process because widening of gap distance may

lead to leakage of the sample through the gap. Therefore, the apparatus has a servo-controlled motor for automatic gap control (marked as B in **Fig. 4**) and it has an electric transducer for measuring gap distance, which is the input sensor to the servo-controlled motor on the order of 1/1000mm. With the mechanism, the gap distance can be kept constant with enough precision during tests.

2.2. Monitoring Instruments

Monitoring instruments

Normal load on the sample is measured with a load cell set in the central axis (D in **Fig. 4**). The normal load acting on the shear plane pushes the upper half of the sample box upward as its reaction. The upward force is transmitted to the loading unit (the shaded part of **Fig. 4**) which is attached to the base through the load cell D. Counter weight is loaded to keep the force acting to the load cell D always in the tensile side. Shear resistance of the sample is measured with the load cell E (**Fig. 4**). Assuming that the shear stress is distributed uniformly on the shear plane, the shear stress is calculated from the shear load measured by the load cell E. Vertical displacement of the loading plate (variation of sample height) is measured with the dial gauge F (in **Fig. 4**). Shear displacement is measured with a rotary electric transducer which makes contact with the outside of the lower part of the sample box. Shear speed at the midst of the shear plane is calculated from this monitored shear displacement.

All these measured parameters (normal load, shear load, sample height and shear displacement) are output as electric voltages through amplifier units. All values are displayed in the digital panels of the amplifier box and the time-variation of the values is continually recorded by a 4-channel pen-recorder. It was confirmed that no high-frequency noise was observed. Thus, the values were sampled at the rate of 1.4 times per a second and put into the computer through an A/D converter. The stress path of the normal stress and

shear stress is plotted on the computer display and the values are saved in the disk.

Calculation of normal stress and shear stress

Normal stress σ (kgf/cm^2) is calculated from:

$$\sigma = \frac{F_n}{\pi(r_2^2 - r_1^2)} + \gamma_t \cdot h_{up}$$

where F_n: normal load acting on the shear plane in the midheight of sample that is measured by the load cell (D in **Fig. 4**), r_1: inside radius of the sample box, r_2: outside radius of the sample box, γ_t: total unit weight of the sample, and h_{up}: sample height above the shear plane (about 3~4cm).

$\gamma_t \ h_{up}$ is at most 0.008kgf/cm^2, while the normal stress loaded on the sample in this study was between 0.5 and 3.8kgf/cm^2, so the second term ($\gamma_t \cdot h_{up}$) was almost negligible. Shear stress τ (kgf/cm^2) is calculated from the equation of rotational torque (**Fig. 6**);

$$\int_{r_1}^{r_2} 2\pi r \ \ r\tau dr = RFs$$

$$\tau = \frac{3RFs}{2\pi(r_2^3 - r_1^3)}$$

where, r_1, r_2 : the inside and outside radii of the sample box, Fs : shear load measured by the load cell, and R : distance between the load cell and the axis of rotation of the sample box.

The error in measurement of normal stress that may be caused by contact force of rubber edges was tested by varying gap ±0.02mm from the preset value for an empty sample box. The result shows that the fluctuation of the contact force when the gap control is working was less than 0.78kgf (0.0015kgf/cm^2). Thus, these errors were ignored in experimental results. Another possible error in normal stress due to self-weight of loading unit was eliminated by employing an appropriate value of counter weight.

Shear load caused by the friction of rubber edges was measured to be 1.6~4.0kgf (0.01~0.02kgf/cm^2) by rotating the sample box without filling sample materials. However, the shear load during the test series was practically negligible probably because the increase in load due to the rubber friction was cancelled out by the friction force acting in the rotary joint (I in **Fig. 4**) impeding the rotation of the sample box. Therefore, these effects on the measured values were ignored in dealing with experimental results. The total dynamic range of data-acquisition system is 60dB, and it corresponds to 0.004 kgf/cm^2 for normal stress resolution, 0.003 kgf/cm^2 for shear stress resolution.

2.3. Samples and Test Procedures

2.3.1. Test Series A

In Test Series A, normal stress is continuously changed during one continuous shearing at a certain speed. The characteristics of this test are 1) one continuous test gives one failure envelope, 2) the influence of normal stress on the shear resistance is visualized in the curve of the failure envelope.

Because the variation of the friction angle during shear seemed to depend on the material property of the soils, the following three samples having different characteristics were chosen (**Table 2–1**).

1) Glass beads (2mm diameter)

   The sample is not crushed during shear under the tested normal stress (0.1 ~ 3.8kgf/cm^2), and consists of uniform, well-rounded grains.

2) The Toyoura standard sands

   These sands are beach sands, so are naturally sorted and ground during water-transport.

3) Bentonite clays

These samples are commercial clays used in boring and other civil engineering works. Montmorillonite clays are predominant and the grain shape is platy.

Glass beads and the Toyoura standard sands are frequently used as references for soil tests. The sample was compacted inside the sample box to 6~7cm in height with a steel bar. Compaction is carefully executed to make a homogeneous sample. The upper unit including the loading plate and air pistons are then set. Before shearing, each sample was consolidated with normal stress of 3.8kgf/cm^2 Progress of consolidation was monitored on pen-recorder by dial gauge for measuring the sample height. Consolidation was completed quickly, because all samples were dry as stated in the Introduction.

After the consolidation, the normal stress was changed to 0.5 kgf/cm^2 The slowest gear was then connected to the servo-controlled motor, and rotation was started at 0.01 cm/sec. After the sample passed the peak and reached the residual state, the normal stress was increased gradually up to 3.8kgf/cm^2 at a constant rate, and then gradually decreased again to 0.5 kgf/cm^2 and finally the rotation was stopped. During the shear test, stress path (relation between normal stress and shear resistance) was plotted continuously on the computer display in real time.

After the test at 0.01cm/sec, tests at shear speeds of 0.1, 1, 10, and 100 cm/sec were carried out without replacing of samples. The procedure of each test was the same except for the test of 100 cm/sec. It is difficult to keep such high speed shearing for tens of minutes from various aspects such as leakage of sample, wearing of rubber edges and gears. Hence, the test at 100cm/sec was done under a constant normal stress condition for some seconds, choosing four discrete normal stresses. After the completion of each shear test, the upper unit of the apparatus, the upper part of the sample box and the sample above the shear plane were removed and shearing plane of the sample was closely observed.

Shear resistance versus normal stress was plotted using the data saved in the disk (as shown in **Fig. 7, 8–1, 9–1**). Friction angles and cohesions are determined by linear

regression in the Mohr-Coulomb law as expressed below and the lines are drawn in the figures. Cohesion was in general less than 0.05 kgf/cm^2 and the materials may be regarded as cohesionless[27]. In the following test series all data will be treated as those for cohesionless materials. The correlation coefficient was larger than 0.998 (see Appendix A for detail).

$$s = c + \sigma \tan \phi_m$$

Where, s: shear resistance, ϕ_m: friction angle during shear, c: cohesion.

According to the real time monitoring of the stress path on the computer display, the stress path (the shear resistance envelope) were straight in the increasing normal stress before the tests of Bentonite clays. Then, monitoring to obtain the shear resistance envelope was chiefly focused to the increasing normal stress in the glass beads and the Toyoura standard sands.

However, the stress path in the first test of Bentonite clays was unexpectedly observed to curve in the increasing process of normal stress and almost straight in the decreasing normal stress. Then, the monitoring to obtain the shear resistance envelope was chiefly focused to the decreasing normal stress in the Bentonite clays.

In Appendix A, the processes of normal stress used in the linear regression are presented in the tables. The difference between the friction angle obtained from the increasing process and the friction angle from the decreasing process was 0.1~0.3 degrees.

2.3.2. Test Series B

In this series of tests, normal stress was kept constant during a test using a servo-controlled air regulator. Shear displacement until 100m was given in one continuous test. The characteristics of this test is 1) the influence of shear displacement on the friction angle is well presented, 2) shearing under a constant normal stress is very similar to the motion of natural landslides. The following three samples were used (**Table 2–2**).

1) Glass beads (2mm diameter)

Glass beads which are quite round and not crushed during shear in the apparatus.

2) The Shirakawa river sands

The Shirakawa river sands which were taken from the Shirakawa river in Kyoto and air-dried. The sample was sieved so that the grain size is between 0.84~9.52mm. The sands are weathered granite which are naturally sorted and ground during transportation by water.

3) The Zentoku landslide soils

The Zentoku landslide soils which were weathered crystalline-schist soils taken in the Zentoku landslide[20),21)] in the crystalline-schist area in the Shikoku island. The soils contain many slender grains, and are regarded to be weathered soils, and not sorted nor ground by water transportation. The samples were air-dried and sieved to remove grains greater than 9.52mm. Consolidation procedures were the same as in Test Series A.

The conditions of Test Series B were : under constant normal stress, the sample is sheared in three stages. The first stage is at 0.01cm/sec up to shear displacement of 10cm, the second is at 1cm/sec up to 10^3cm, and the final stage is at 10cm/sec up to 10^4cm. Normal stresses for the tests are 1.0kgf/cm^2 and 3.0kgf/cm^2 During each test, the friction angle and the variation of the sample height were successively measured and recorded by computer.

After Test Series B, an additional test was carried out to distinguish the influence of shear speed from the shear distance as described in section 4.1.

3. TEST RESULTS

3.1. Results of Test Series A

3.1.1. 2mm Glass Beads and the Toyoura Standard Sands

The test result of dry 2mm glass beads is shown in **Fig. 7**. The friction angle during shear at 0.01, 0.1, 1, and 10cm/sec is almost same, 21.8°. Distinct increment or decrement of the friction angle with shear speed is not observed, though a slight variation less than 0.5 degrees is found. The cohesion is nearly zero. According to careful observation of the sample after shear, no indication of grain crushing was found.

Fig. 8–1 shows the test results of the Toyoura standard sands. The friction angle during shear increased from 31.4° to 33.9° when the shear speed was changed to 0.01, 0.1, 1, 10, and 100cm/sec in this order. Thereafter, tests were continued at the slower speeds; 1cm/sec, 0.1cm/sec, and 0.01cm/sec. The tests with reduced the shear speed were carried out in order to examine whether the shear friction depends only on the shear speed or not. Change of the sample height (change of the sample volume) and the friction angle versus shear speed during this whole test are plotted in **Fig. 8–2**. The plot numbers in this figure give the order of the ring shear test. The friction angle during shear tends to increase during the tests 1~5 and were almost constant (or slightly decreasing) during 5~8. Sample height increased until test 3, and then continued to decrease during tests 4~7. The increasing process was indicative of the positive dilatancy of the sample. The negative dilatancy in the decreasing process seemed to be chiefly owing to crushing of the sample. This is supported by the comparison between the grain size distributions of the samples before the test of **Fig. 8–1** and after the test as shown in **Fig. 8–3**. Finer grains (< 0.05mm) which did not exist in the sample before the ring shear test appeared in the distribution curve after the test. In the tests of the Toyoura standard sands, the shear zone was not visible, which situation is similar to that for glass beads, but different

from those for other natural samples. Therefore, in the Toyoura standard sands case, the sample after the test for the grain size distribution could not be taken only from the shear zone.

3.1.2. Bentonite Clays

The test results of the air-dried Bentonite clays (**Fig. 9–1**) showed great difference in friction angle with the change of shear speed. The friction angle was 28.4° at the first cycle of shear test at the shear speed of 0.01cm/sec. It then varied as 34.2° at 0.1 cm/sec, and 35.0° at 1cm/sec. After the test at 10cm/sec, a test at 0.01cm/sec was performed to examine whether the friction angle depends on only the shear speed or not. But the friction angle did not decrease and remained almost the same as that at 10cm/sec. This was a trend similar to the tests on the Toyoura standard sands. **Fig. 9–2** shows the full stress paths of the two cycles of shearing at 0.01cm/sec and 0.1cm/sec of the test shown in **Fig. 9–1**, in which almost linear part of the stress paths at the decreasing normal stress are plotted because the stress paths in the increasing process was not straight as written below. **Fig. 9–2** clearly visualized the variation of the friction angle during shear. The friction angle seems to change continually probably because of crushing of the sample. To know the variation of friction angle with the process of shear displacement, $\tan^{-1} s/\sigma$ (s: shear resistance, σ: normal stress) is plotted in **Fig. 9–3**. This is justified because the shear resistance envelope was straight and no significant difference between secant and tangential coefficients was observed. **Fig. 9–3** represents the variation of the sample height, the friction angle during shear, normal stress and shear resistance in the cycle of the shearing at 0.1cm/sec of **Fig. 9–2**. In this figure, the abscissa is the shear displacement and the ordinate shows the normal stress, the shear resistance, the sample height and the friction angle during shear. The normal stress was increased up to 3.5kgf/cm^2 at a constant speed and remained at 3.5kgf/cm^2 for a while, and then was decreased to 1.2 kgf/cm^2 again. The shear resistance also changed in proportion to the normal stress.

Most remarkable is the behavior of the friction angle during shear. It increased with the increase of normal stress (during the shear displacement of 0~20cm) and also kept increasing during a constant normal stress of 3.5kgf/cm^2 (shear displacement : 20~30cm). And when the normal stress decreased, the friction angle during shear remained constant (shear displacement : 30~47cm). The sample height decreased during shear and did not fully recover the initial height at the end of the test. On the shear plane after the ring shear test of **Fig. 9–1**, many striations and many finely ground grains were observed. **Photo. 3** shows the situation of the sample after the test was completed and the upper half of the sample was removed. A smooth shear plane is found in the Photo. Multiple layered shear planes were observed in a zone of the middle of the sample, which were presumably formed during shear under the changing normal stress. Bentonite clays in this shear zone were harder than those before the test. Such shear zone was not observed in the case of Toyoura standard sands probably because crushed fine grains moved downward through voids. The comparison of the grain size distributions (**Fig. 9–4**) of the Bentonite clays sample before the test and the sample taken from the shear zone after the test of **Fig. 9–1** exhibits the effects of grain crushing through shearing. The difference between the maximum and the minimum friction angle is 0.3 degrees in the tests of glass beads, however the difference of the friction angle in the Toyoura standard sands and the Bentonite clays is 2.5~6.6 degrees. It is one order greater than that in the glass beads. The cause of difference is considered to be related to grain crushing during shear in the Toyoura standard sands and the Bentonite clays as discussed in the section 4.

3.2. Results of Test Series B

3.2.1. 2mm Glass Beads

Variation of the friction angle during shear and the sample height in the Test Series B on 2mm glass beads under the constant normal stress of 1.0kgf/cm^2 and 3.0kgf/cm^2 are

shown in **Fig. 10–1**. Here, the friction angle during shear is expressed in the form of the ratio between the shear resistance and the normal stress, because of the same reason as in the case of Bentonite clays. The friction angle during shear decreased at the beginning of shear speed of 1cm/sec (probably due to gear change), and seemed to be almost constant in about 50cm$\sim$ 10^3cm shear displacement. Both of the sample height and the friction angle began to decrease in the test at 10cm/sec.

The variations of sample height and the friction angle at $10, 10^3, 10^4$cm shear displacement under two normal stress conditions (σ =1.0, 3.0kgf/cm^2) are presented in **Fig. 10–2**. Each plot is the variation from the value at the shear displacement of 10cm.

The sample height does not change in $10 \sim 10^3$cm shear displacement, but it decreases in $10^3 \sim 10^4$cm shear displacement. The friction angle during shear decreases with the shear displacement. No grain crushing was observed during the shear, so that the major reason why the friction angle decreases at higher shear speed was conjectured to be grains aligning along concentric paths and interlocking of grains along the shearing path decreases. This will be discussed later in section 4.

3.2.2. The Shirakawa River Sands

The result of the test under the normal stress of 3.0kgf/cm^2 is shown in **Fig. 11–1**. Friction angle corresponding to peak strength was observed at about 1cm of shear displacement and it reached residual strength at about 2cm or so. However, the friction angle during shear began to increase at $10^2 \sim 10^4$cm shear displacement and finally the friction angle increased by 1.4° Sample height began to increase firstly, then turned to decrease at about 2 cm of shear displacement and continued to decrease until 10^4cm. The increment of sample height due to positive dilatancy is 0.8mm, but the decrement of the sample height due to negative dilatancy following it is about 9mm. Taking the initial height of sample of about 76mm into consideration, this great shrink of volume will be resulted from grain crushing. This is supported by the grain size distribution in **Fig. 11–**

3. **Fig. 11–2** shows the results of the tests under the normal stress of 1.0kgf/cm^2 and 3.0kgf/cm^2. Both test results show that the decrease of sample height and the increase of friction angle proceeded with shear displacement.

Fig. 11–3 shows the comparison of the grain size distributions of the samples after the tests of **Fig. 11–2** which were taken from the shear zone, and of the sample before the test. **Photo. 4–1** shows the Shirakawa river sands in the sample box after the test of **Fig. 11–2** in which the upper portion of the sample above the shear plane is removed. **Photo. 4–2** shows the sample in the shear zone (right) and the sample before the test (left). Grain size of the sample after the test became smaller, which clearly shows that grain crushing occurred at the shear plane during shear, and it was greater under higher normal stress.

3.2.3. The Zentoku Landslide Soils

The result of the test under the normal stress of 3.0 kgf/cm^2 is shown in **Fig. 12–1.** **Fig. 12–2** shows the test results under the normal stresses of 1.0kgf/cm^2 and 3.0kgf/cm^2 In the test under 3.0kgf/cm^2 normal stress, both of the sample height and the friction angle decreased. In the test under 1.0kgf/cm^2 normal stress, the sample height decreased until the end of the test, but the friction angle during shear first increased in $10 \sim 10^3$cm shear displacement, then decreased in $10^3 \sim 10^4$cm shear displacement.

Photo. 5–1 is the Zentoku landslide soils in the sample box after the test under σ = 3.0kgf/cm^2 in **Fig. 12–1.** **Photo. 5–2** shows the sample in the shear zone of **Photo. 5–1** (right) and the sample before test (left). **Fig. 12–3** shows the grain size distributions of the samples before the test and the samples in the shear zone after the tests of the Zentoku landslide soils. The portion of finer grains apparently increased during the test. However, the grain size distribution after the test under σ =3.0kgf/cm^2 is almost same as that in the case under σ =1.0kgf/cm^2

4. DISCUSSION

Variation of the friction angle during shear was observed in the two series of ring shear tests presented in the previous section. The cause of the increase of the friction angle during shear seemed to be grain crushing during shear. On the other hand, the results on 2mm diameter glass beads and the Zentoku soils in Test Series B suggest that there are other reasons which cause the decrease of friction angle during shear. In the following, the mechanism of the variation of the friction angle during shear and also the probable influences of the variation of the friction angle during shear upon the motion of real landslides are discussed.

4.1. Increment of the Friction Angle during Shear Due to Grain Crushing

Fig. 9–3 shows one cycle of test at a shear speed of 0.1cm/sec on a dry Bentonite sample. In the figure, the friction angle increased during the increasing process and at the peak value of the normal stress. However, the friction angle remained constant even after the normal stress was decreased. The sample height at the end of the cycle of the test was about 1mm less than that at the start of the test. Because the sample box is restricted not to deform horizontally, variation of the sample height means variation of the total sample volume. Hence, the decrease of the sample height means the decrease of the void ratio of the sample. The cause of decrease of the sample height should not be consolidation in the ordinary meaning because consolidation had been already completed before shearing, and moreover a cycle of test at 0.01cm/sec under the same normal stress range preceded this cycle of test. **Fig. 9–4** shows the grain size distributions of the Bentonite sample taken from the shear zone after the test of **Fig. 9–1** and the sample before test. In this figure, finer grains increased after the test, and it implied that grain crushing occurred during

shear. Although **Fig. 9–4** is not from the sample just after the test at 0.1cm/sec, grain crushing was estimated to have occurred through the whole shear displacement, because the loaded normal stress was constant. It will be understood that the finer grains produced by grain crushing get into the void in the sample, decrease the void ratio, and increase the friction angle during shear.

In Test Series B on the Shirakawa river sands, **Fig. 11–2** shows that the increment of the friction angle as well as the decrement of the sample height from the values at the shear displacement of 10cm, progress with shear displacement. **Fig. 11–3** shows that the finer grains were produced by grain crushing during shear. It is supposed that the finer grains thus produced decreased the void ratio and resulted in the increase of the friction angle during shear. The decrement of sample height was same in the cases of σ =1.0, 3.0kgf/cm^2 in **Fig. 11–2** though the test at σ = 3.0kgf/cm^2 had caused more grain crushing. This will be due to the lower void ratio in the case of σ = 3.0kgf/cm^2

Examination of the influence of shear speed

The shear speed in the Test Series B was increased as 0.01cm/sec →1cm/sec →10cm/sec in steps. Thus, it is not very clear whether the observed variations of the friction angle during shear was due to the shear speed or the shear displacement. In order to distinguish the effect of shear speed from the effect of the shear displacement, the following test on the Shirakawa river sands was carried under the constant normal stress of 3.0kgf/cm^2 Shear speed was alternatively changed to 1.0cm/sec and 10cm/sec as shown in **Table 3**, so that the friction angle during shear of both speeds might be obtained at each step of similar shear displacement of 5, 10, 50, and 100m. In **Fig. 13** the final values of the friction angle during shear and the sample height at each speed are plotted as the variation from those values at the shear displacement of 10cm. Neither the friction angle during shear nor the sample height exhibited any difference depending on shear speed. The final value of the increment of friction angle during shear at the shear displacement of 10^4cm was 1.2° in **Fig. 13** and 1.3° in the test of σ =3.0kgf/cm^2 in **Fig. 11–2**. The difference due

to different testing methods is negligible. Thus, it can be concluded that both of grain crushing and the increase of the friction angle during shear progress mostly with the shear displacement.

4.2. Decrement of the Friction Angle during Shear Due to Grain Alignment and Grain Re-orientation

4.2.1. Grain Alignment

In the test of glass beads (**Fig. 10–2**), the friction angle during shear under the normal stress of 1.0kgf/cm^2 and 3.0kgf/cm^2 decreased with the decrement of sample height. However, upon a close observation of the sample after the test no crushed grains were found in the sample. This implies that no grain crushing during shear occurred and no influence by this effect existed. Because the tested glass beads are spherical, no re-orientation could occur. The only possible reason for the decrease of both of the sample height and the friction angle during shear is the grain alignment along the concentric shear paths in the sample box, as illustrated in **Fig. 14**. When glass beads of uniform diameter align along concentric paths along shear direction, vertical fluctuation of the glass beads to get over other beads (dilatancy) during shear becomes small, and the friction angle during shear will decrease. The sample height of well-aligned grains as illustrated in **Fig. 14** seems to be smaller than that of randomly aligned grains.

4.2.2. Grain Re-orientation

The tests of **Fig. 12–2** on the Zentoku landslide soils showed that the friction angle during shear decreased in the shear displacement of $L = 10 \sim 10^3$cm and $10^3 \sim 10^4$cm under σ =3.0kgf/cm^2, and it decreased in the shear displacement of $L = 10^3 \sim 10^4$cm under σ =1.0kgf/cm^2 It is obvious from **Fig. 12–3** that grain crushing occurred during shear. Grain crushing is expected to increase the friction angle during shear according

to the previous discussion. It was not the case for the Zentoku landslide soils. The reason for the friction angle during shear decreasing in spite of the occurrence of grain crushing may be the effect of grain re-orientation. The Zentoku landslide [20),21)] is located in a crystalline-schist area of Shikoku island, Japan, where the grains of the soils in this landslide consist of weathered crystalline-schist, the grains of which are slender. Bishop[22)] regarded the cause of the decrease of the strength of clays in the residual state as the influence of re-orientation of clay particles adjacent to the shear plane. The soils of the Zentoku landslide were not clays, but of slender grains. Grain shape was observed by SEM (Scanning Electron Microscope) and mineral microscope. Both observation showed that the fine grains of the Zentoku landslide soil were also slender. It can be considered that grain re-orientation occurred during shear in the shear zone, though an undisturbed sample from the shear zone was not directly observed by microscope or SEM. The image of re-orientation is illustrated in **Fig. 15** referring to the figure of re-orientation of clays during shear[23)].

4.2.3. Difference between the Grain Alignment and the Grain Re-orientation

It is clear that grain re-orientation cannot take place in glass beads because of their spherical shape. As Illustrated in **Fig. 14**, grain alignment along the shear direction will occur necessarily in grains having the same or similar diameters. On the other hand, in the soils which have wide grain size distribution, grains are difficult to align and keep it during relative motion. The glass beads have completely the same diameter, but the Zentoku landslide soils consist of grains having a wide range of diameters as shown in **Fig. 12–3**. Well-graded soils such as the Zentoku landslide soils would not exhibit the influence of grain alignment so much. However, grains having anisotropic shapes (slender or platy) of the Zentoku landslide soils would exhibit the influence of grain re-orientation.

The Shirakawa river sands have characters between those of glass beads and the Zen-

toku landslide soils in the aspects of grain-shape and grain-size distribution. Their grain shape is angular, but neither slender nor platy, and may be regarded to be nearly spherical. Furthermore, the grain size of the Shirakawa river sands were almost $1 \sim 2$mm before the test, and about a half of grains after the test were still $0.5 \sim 2.0$mm and rather uniform as shown in **Fig. 11–3**. Therefore, the Shirakawa river sands may be susceptible to grain alignment.

4.3. The Mechanism of Variation of the Friction Angle during Shear

The variation of the friction angle during shear $\Delta\phi_m$ is resulted from crushing, alignment and re-orientation of grains during shear. Double effect of two factors and the influence of material strength on grain crushing are examined here.

4.3.1. Double Effect of Grain Crushing and Grain Re-orientation

In the test under the normal stress of 1.0kgf/cm^2 of the Zentoku landslide soils (**Fig. 12–2**), the friction angle during shear increased during the shear displacement of $10 \sim 10^3$cm, but began to decrease during $10^3 \sim 10^4$cm. This may be interpreted as follows: during the shear displacement of $10 \sim 10^3$cm, the increment of the friction angle by grain crushing was greater than the decrement of the friction angle by grain re-orientation. However, as suggested by the variation of the sample height, grain crushing was completed before 10^3cm and it did not progress further. Hence the influence of re-orientation became evident beyond the shear displacement of 10^3cm.

The friction angle during shear decreased monotonically in the test under 3.0kgf/cm^2 The decrement of the friction angle by grain re-orientation is considered to have been greater than the increment by grain crushing in the whole range of shear displacement. The progress of grain re-orientation seems to be affected by the normal stress.

4.3.2. Double Effect of Grain Crushing and Grain Alignment

In the tests of the Shirakawa river sands (**Fig. 11–2**), the increment of the friction angle under 3.0kgf/cm^2 normal stress is smaller than that under 1.0kgf/cm^2, though grain crushing under 3.0kgf/cm^2 should be greater than that under 1.0kgf/cm^2 as supported by the grain size distributions in **Fig. 11–3**. It can be interpreted that grain alignment or grain re-orientation appeared strongly at shearing under higher normal stresses.

The Shirakawa river sands are naturally sieved, weathered, granite grains, most of which are mostly quartz grains, with shapes that are neither slender nor platy. Thus, it is not probable that they are subjected to re-orientation. Taking their relatively uniform grain size (mentioned at the end of section **4.2.**) into consideration, it will be reasonable to interpret that the influence of grain alignment became somewhat dominant to that of grain crushing under higher normal stresses.

4.3.3. Examination of Material Strength

Both in **Fig. 13** and in **Fig. 11–1** the sample height decreased, but approached a certain limiting value. This implies that there is a limit to the degree of grain crushing corresponding to a test condition. Comparing the grain size distributions of the Shirakawa river sands (**Fig. 11–3**) with those of the Zentoku landslide soils (**Fig. 12–3**), a difference in grain crushing is found. In the Zentoku landslide soils, all crushable grains could be crushed out under the normal stress of 1.0kgf/cm^2 The extent of grain crushing was almost same under the higher normal stress of 3.0kgf/cm^2 On the contrary, grain crushing under 3.0kgf/cm^2 in the Shirakawa river sands was more extensive than that under 1.0kgf/cm^2 as shown in **Fig. 11–3**. It means that grains not crushed under 1.0kgf/cm^2, were crushed under 3.0kgf/cm^2 This is likely caused by the characteristics of weathered granite grains which consist of various minerals such as quartzs, feldspars, and others. Among the tested materials, only the glass beads were not crushed under the tested normal stress. But even the glass beads will be crushed during shear under normal stresses

exceeding their strength. Hence, the extent of grain crushing depends on the material strength as well as the normal stress applied and the shear displacement.

4.4. Variation of the Friction Angle during Shear in Natural Landslides

What effect does the variation of the friction angle during shear studied here have on the motion of real landslides ? Some probable situations are examined in the following.

4.4.1. Influence of Grain Crushing

Grain crushing is considered to occur when stress is higher than the material strength. Normal stress corresponds to the depth of the landslide mass above the sliding surface. The depth of the landslide mass corresponds to the landslide volume, so that the variation of the friction angle during shear due to grain crushing will appear more often in such landslides that the normal stress at the sliding surface is high enough to cause grain crushing. The shear displacement in the ring shear tests in this paper corresponds to the travel distance in landslides. When a landslide moves, grain crushing during motion at the sliding plane will progress with the travel distance up to a certain value.

Grain crushing will appear in a newly activated landslide more than in a re-activated one. Since shear strength increases with the progress of grain crushing, it will work to stabilize the landslide motion. Even though the increment of the friction angle by grain crushing is not so great, it may have an effect on the motion of landslides in a marginal safety factor.

When grain crushing occurs in a saturated and undrained condition, the situation is quite different. **Fig. 16**[24] shows the stress path of the ring shear test on a dried torrent deposits sample of the Denjo river under constant volume condition. The numerical values in the figure show the shear distance in cm. The constant volume condition in the ring shear test almost corresponds to the undrained condition of fully saturated samples in a triaxial

test. Because pore water is almost incompressible compared with the compressibility of soil-structure, the total volume of soils including pore water must be kept constant if pore water will be kept in an undrained condition. The main difference between the undrained condition of a fully saturated sample and the constant volume test is the negative pore pressure during dilation of the sample. If the soils tend to dilate during shear, a negative pore pressure will be generated in the triaxial test. However, its maximum value is minus one atmospheric pressure (about 1.0kgf/cm^2) because the maximum suction pressure in the vacuum state is 1 atm. On the other hand, the effective stress in a constant volume test can increase as much as the sample tends to dilate. In **Fig. 16**, the sample tends to dilate until the shear displacement of 1.88cm, then tends to shrink and the effective stress decreases. This shrinkage must be the effect of grain crushing. This behavior is similar to that of the Shirakawa river sands shown in **Fig. 11–1**, where the peak of dilatancy appeared at the shear displacement of about 2cm and later the sample shrank by grain crushing.

Hence, if the undrained condition or a semi-undrained condition is kept during shear, the shear strength must decrease to a great extent due to grain crushing (e.g. in the case of **Fig. 16**, the shear strength in the constant volume condition (corresponding to the undrained condition) is 0.25kgf/cm^2 at 650cm shear displacement, which is about 1/7 of the drained shear strength (1.75kgf/cm^2) at the normal stress 2.5kgf/cm^2) because grain crushing cause the decrease of the sample volume. It should result in promoting the motion of landslides. This effect would have appeared in the initiation of the Ontake landslide which slid on the crushable volcanic soils. When a landslide moves on a saturated slope or torrent deposits and the landslide mass is large enough to generate grain crushing, grain crushing may have a great effect in the motion of landslide.

4.4.2. Influence of Grain Re-orientation and Grain Alignment

In this study, the influence by re-orientation appeared in the Zentoku landslide soils.

Re-orientation will not appear when the grains are not platy. The shape of the grains are due to mineralogical characteristics of soils. Furthermore, minerals keep their original and characteristic shapes even if they are crushed. Thus, in a landslide in which the soils contain long or platy minerals, re-orientation will progress regardless of grain crushing. In **Fig. 12–2**, the decrement of the sample height almost ceased for the shear displacement greater than 10^3cm. The decrement of the friction angle during shear became apparent after the sample height ceased to decrease, because grain crushing increases the friction angle and it cancels the decrement of the friction angle due to grain re-orientation.

The Zentoku landslide has moved repeatedly. The reason for the repeated motion has been explained by excess pore pressure in the sliding surface due to heavy rainfall.[20] It means that it has not been stabilized, though the displacement of landslide mass geometrically should have increased its stability. The reason (namely the mechanism), for this repeated motion may be in part explained by grain re-orientation during shear which will appear over 10~100m of shear displacement. **Fig. 12–2** suggests that re-orientation is greater under higher normal stresses. In Japan, repeated motion of landslides is typically observed in large crystalline-schist landslides and also in large tertiary-mudstone landslides. This may be due to their grain shape ("slender" in the crystalline schist landslide soils and "platy" in the tertiary-mudstone landslide soils in which montmorillonite clays are predominant) and their greater normal stress in respect to grain re-orientation.

5. CONCLUSIONS

1. High-speed high-stress ring shear tests were carried out using granular materials to investigate the friction angle during shear, especially to examine whether it will vary or not in the progress of shearing because some previous researches showed variation of the friction angle during shear, but others did not. Results of this study showed that the friction angle during shear varied except for 2mm diameter glass beads. It

increased for some samples, and decreased for the others with the progress of shear displacement.

According to the test results, the variation of the friction angle during shear is much affected by the shear displacement and also by the normal stress, but hardly by the shear speed.

2. Three causes for the variation of the friction angle during shear have been found:

   A) Grain crushing produces finer grains and necessarily decreases the void ratio of the material in the shear zone. The decrement of the void ratio of the material results in the increment of the friction angle during shear.

   B) When the material includes many slender or platy grains, grain re-orientation parallel to the shear plane causes the decrement of the friction angle during shear.

   C) When the major portion of grains are uniform in size, grain alignment along the shear direction may occur, causing the decrement of the friction angle during shear.

   The variation of the friction angle during shear ($\Delta\phi_m$) consists of the above-mentioned three effects.

3. In real landslides, grain crushing will occur in larger landslides compared with their material strength, and it will increase the friction angle during shear. This may work for stabilization of landslides under the drained condition. On the contrary, when grain crushing will be caused in landslides under the undrained condition, it will necessarily generate excess pore pressure due to shrinkage of soils and result in a great decrease of shear resistance.

4. Grain re-orientation will appear in landslides in which the shape of grains is slender such as in crystalline-schist landslides, or platy such as in tertiary-mudstone landslides, and will decrease the friction angle with the progress of shear displacement. Generally a landslide recovers its stability by its motion. However, when re-orientation of grains occurs, the recovery of stability will be cancelled by the decrease of strength accom-

panying re-orientation. Therefore, some landslides are not easily stabilized, but may move repeatedly. This explains partly why large landslides in the crystalline-schist areas and in the tertiary-mudstone area in Japan move so repeatedly.

ACKNOWLEDGMENT

The author thanks Professor Michiyasu Shima, the Disaster Prevention Research Institute, Kyoto University, for his supervision and support to this research. The author also wishes to express sincere appreciation to Associate Professor Kyoji Sassa, the Disaster Prevention Research Institute, Kyoto University, for his kind guidance and encouragement during study. Thanks are also due to Professor Kazuo Okunishi, the Disaster Prevention Research Institute and Associate Professor Yoshimasa Kobayashi, the Geophysical Institute, Kyoto University for their helpful comments.

REFERENCES

1) Inokuchi, T.: The Ontake Rock Slide and Debris Avalanche Caused by the Naganoken-Seibu Earthquake, 1984, Proc. IVth International Conference and Field Workshop on Landslides, 1985, pp. 329–338.

2) Wang, S., Z. Zhang, Z. Zhan and H. Liu: On the Characteristics and Dynamics of the Catastrophic Mount Sale Landslide, Kansu, China, Proc. IVth International Conference and Field Workshop on Landslides, 1985, pp. 429–432.

3) Cruden, D.M. and J. Krahn: Frank Rockslide, Alberta, Canada, in Rockslides and Avalanches, 1, ed. by B. Voight, Elsevier, 1978, pp. 97–112.

4) Scheidegger, A.E.: On the Prediction of the Reach and Velocity of Catastrophic Landslides, Rock Mechanics, Vol. 5, 1973, pp. 231–236.

5) Hsü, K.J.: Catastrophic Debris Streams Generated by Rockfalls, Geol. Soc. Amer. Bull., Vol. 86, 1975, pp. 129–140.

6) Davies, T.R.H.: Spreading of Rock Avalanche Debris by Mechanical Fluidization, Rock Mechanics, Vol. 15, 1982, pp. 9–24.

7) Melosh, H.J.: Acoustic Fluidization : A New Geologic Process ?, Jour. Geophys. Res., Vol. 84, No. B13, 1979, pp. 7513–7520.

8) Habib, P.: Production of Gaseous Pore Pressure During Rock Slides, Rock Mechanics, Vol. 7, 1975, pp. 193–197.

9) Voight, B. and C. Faust: Frictional Heat and Strength Loss in Some Rapid Landslides, Géotechnique, Vol. 32, No.1, 1982, pp. 43–54.

10) Sassa, K.: The Ontake Debris Avalanches and its Interpretation, Int'l News Letter "Landslide News," No. 1, 1987, pp. 6–8.

11) Sassa, K., H. Fukuoka, J.H. Lee and D.X. Zhang: Measurement of the Apparent Friction Angle during Rapid Loading by the High-Speed High-Stress Ring Shear Apparatus – Interpretation of the Relationship between Landslide Volume and the Apparent Friction during Motion –, Proc. 6th Int'l Symp. Landslides, 1992, (in print).

12) Novosad, J.: Studies on Granular Materials. II. Apparatus for Measuring the Dynamic Angle of Internal and External Friction of Granular Materials, Collection Czech. Chem. Commun. Vol. 29, 1964, pp. 2697–2701.

13) Scarlett, B. and A.C. Todd: The Critical Porosity of Free-Flowing Solids, J. Engng. Ind. Ser. A, Vol. 91, Part 1, 1969, pp.478–488.

14) Bridgwater, J.: Stress-velocity Relationships for Particulate Solids, ASME Paper No. 72–MH–21, 1972, American Society of Mechanical Engineers, 7 pages.

15) Hungr, O. and N.R. Morgenstern: High Velocity Ring Shear Tests on Sand, Géotechnique, Vol. 34, 1984, pp. 415–421.

16) Sassa, K., M. Shima, H. Hiura, A. Nakagawa and A. Suemine: Development of Ring Shear Type Debris Flow Apparatus, Report of Grant-in-Aid for Scientific Research by Japanese Min. of Education, Science and Culture (No.57860028), 1984, 30 pages.

17) Sassa, K., H. Fukuoka, C. Vibert and M. Shima: Development of a High-Speed High-Stress Ring Shear Apparatus and Shear Strength of Reduction at Rapid Loading in Landslides, Annuals, Disaster Prev. Res. Inst., Kyoto University, Vol. 32, No. B–1, 1989, pp.165–182.

18) Vibert, C., K. Sassa, and H. Fukuoka: Friction Characteristics of Granular Soils Subjected to High Speed Shearing, Proc. the Japan–China Symposium on Landslides and Debris Flows, Vol. 1, 1989, pp.295–299.

19) Fukuoka, H., K. Sassa, and M. Shima: Shear Characteristics of Sandy Soils and Clayey Soils Subjected to the High-Speed and High-Stress Ring Shear Tests, Annals of the Disaster Prevention Research Institute, Kyoto University, No.33 B–1, 1990, pp. 179–190 (in Japanese).

20) Sassa, K.: Monitoring of a Crystalline Schist Landslide – Compressive Creep Affected by "Underground Erosion" –, Proc. 4th Int'l Symp. Landslides, Vol. 2, 1984, pp.179–184.

21) Sassa, K., A. Takei, S. Kobashi: The Movement and the Mechanism of a Crystalline Schist Landslide "Zentoku" in Japan, Proc. Int'l Symposium "INTERPRAEVENT 1980", Vol. 1, 1980, pp.85–106.

22) Bishop, A.W., G.E. Green, V.K. Garga, A. Andresen and J.D. Brown: A New Ring Shear Apparatus and its Application to the Measurement of Residual Strength, Géotechnique, Vol. 21, 1971, No. 4, pp. 273–328.

23) Kamon, M., and M. Asakawa: Shearing, in Soil Mechanics, Ch. 9, ed. by the Japan Society of Civil Engineers, Gihodo, 1988, pp.225–262 (in Japanese).

24) Fukuoka, H., K. Sassa, C. Vibert and M. Shima: Shear Characteristics of the Jizukiyama Landslide and the Ontake Debris Avalanche by the High-Speed High-Stress Ring Shear Apparatus, Annals of the Disaster Prevention Research Institute, Kyoto University, No.32 B–1, 1989, pp. 183–195 (in Japanese).

25) Fukuoka, H. and K. Sassa: Variation of the Friction Angle during Shear — Effects of Grain Crushings and Alignment —, Proc. Soviet–China–Japan Symp. and Field Workshop on Natural Disasters, Vol. 1, 1991, pp. 9–20.

26) Fukuoka, H.: Variation of the Friction Angle of Granular Materials in the High-Speed High-Stress Ring Shear Apparatus — Influence of Re-orientation, Alignment and Crushing of Grains during Shear —, Bull., Disas. Prev. Res. Inst., Kyoto Univ., Vol. 41, Part 4, 1991, (in print).

27) Lambe, T.W and R.V Whitman: Shear Strength of Cohesionless Soil, in Soil Mechanics, SI Version, John Wiley & Sons, 1979, pp.137–150.

28) Honma, M. and N. Kasugaya: Dimensional Analysis, Methods of Least Squares, and Empirical Formula, Corona, 1957, 327p. (in Japanese).

APPENDIX A

Linear regression results of the shear resistance envelopes of Test Series A.

2mm glass beads (Fig. 7)

shear speed (cm/sec)	loading process*	$c \pm \Delta c$ ($\times 10^{-3}$ kgf/cm^2)	$\phi_m \pm \Delta\phi_m$ (deg.)	corr. coeff.
0.01	I&D	4.1±0.5	21.69±0.01	0.999
0.1	I&D	20.7±0.6	21.55±0.01	0.999
1	I&D	24.8±1.0	21.89±0.02	0.999
10	I&D	19.7±1.3	21.94±0.03	0.999

Toyoura standard sands (Fig. 8–1 and Fig. 8–2)

shear speed (cm/sec)	loading process*	$c \pm \Delta c$ ($\times 10^{-3}$ kgf/cm^2)	$\phi_m \pm \Delta\phi_m$ (deg.)	corr. coeff.
0.01	I&D	1.3±0.6	31.38±0.01	0.999
0.1	I&D	2.1±0.6	31.77±0.01	0.999
1	I	-9.4±0.7	33.14±0.01	0.999
10	I	-11.6±4.7	33.85±0.10	0.998
100	I	-2.2±3.7	33.67±0.05	0.998
1	I	-2.7±1.3	33.54±0.02	0.999
0.1	I&D	-13.0±0.5	33.70±0.01	0.999
0.01	I&D	-14.0±0.5	33.73±0.01	0.999

Bentonite clays (Fig. 9–1)

shear speed (cm/sec)	loading process*	$c \pm \Delta c$ ($\times 10^{-3}$ kgf/cm^2)	$\phi_m \pm \Delta\phi_m$ (deg.)	corr. coeff.
0.01	D	60.4±0.8	28.40±0.02	0.999
0.1	D	-7.2±0.8	34.22±0.02	0.999
1	D	-32.9±1.7	35.03±0.03	0.999
10	D	-43.2±5.0	34.81±0.12	0.996

$\pm\Delta c$, $\pm\Delta\phi_m$: range of probable error[28)]

corr. coeff. : correlation coefficient between normal stress and shear resistance.

* I : Increasing process of normal stress.

D : Decreasing process of normal stress.

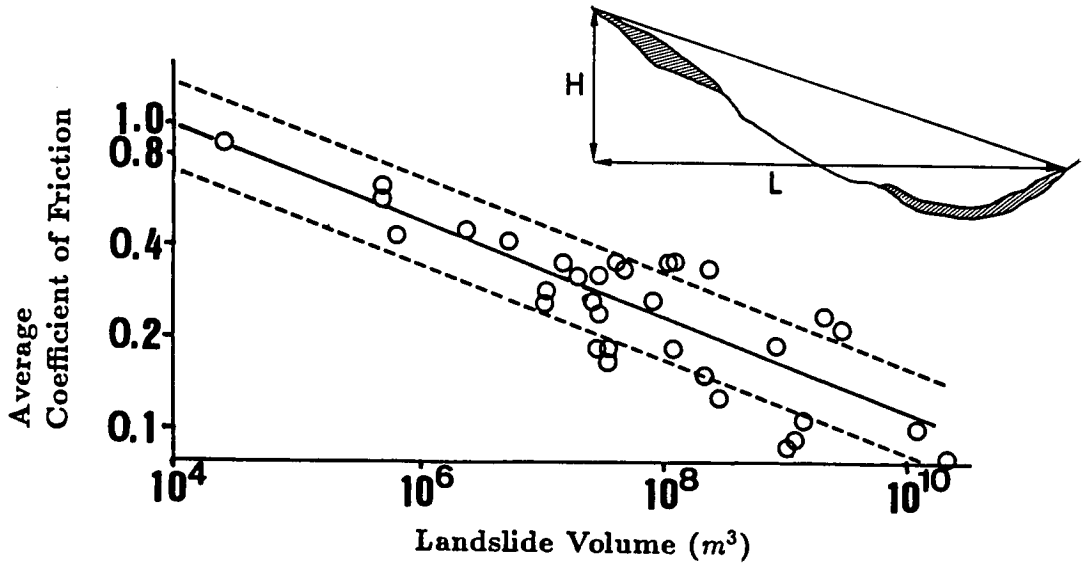

Fig. 1 Scheidegger's diagram on the correlation between landslide volume V and the average coefficient of friction which is total fall height (H) divided by total travel distance (L) (Scheidegger[4]).

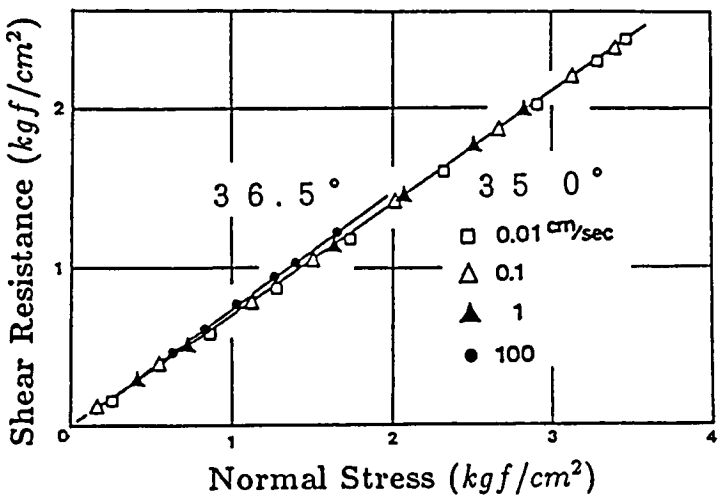

Fig. 2 Result of the high-speed ring shear tests on dry torrent deposit of the Denjo River. Void ratio during shear $e = 0.50 \sim 0.57$ (Vibert et al.[18]).

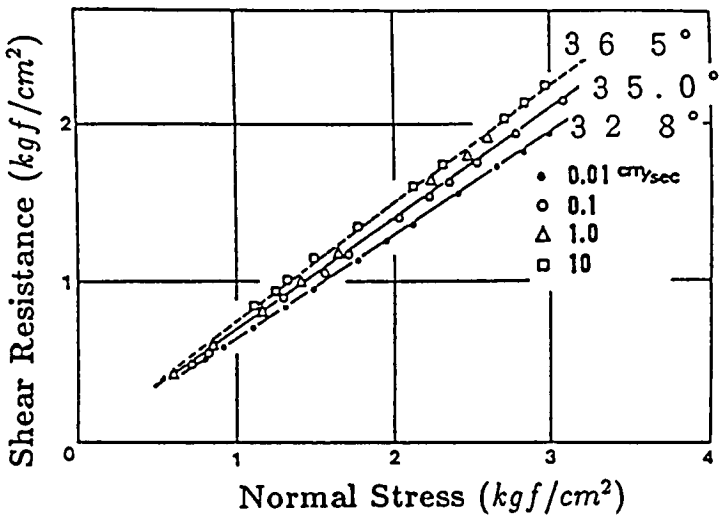

Fig. 3 Result of the ring shear tests on the unsaturated Jizukiyama landslide soil. Degree of saturation= 20.8 ~ 26.1%. Void ratio during shear $e = 0.71 \sim 0.86$. (Fukuoka et al.[24]).

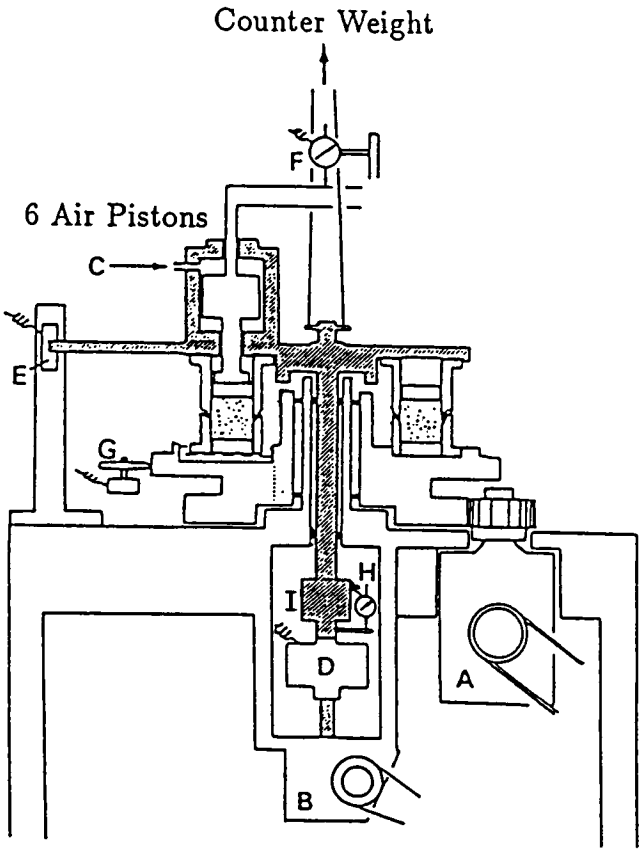

Fig. 4 Schematic Diagram of the High-Speed High-Stress Ring Shear Apparatus. A: pulley connected to the servo-controlled motor for shear, B: pulley connected to servo-controlled motor for gap control, C: pipe connected to the servo-controlled air regulator, D: load cell for normal stress, E: load cell for shear stress, F: electric transducer for volume change measurement, G: rotary electric transducer for shear displacement, H: electric transducer for gap distance, I: rotary joint.

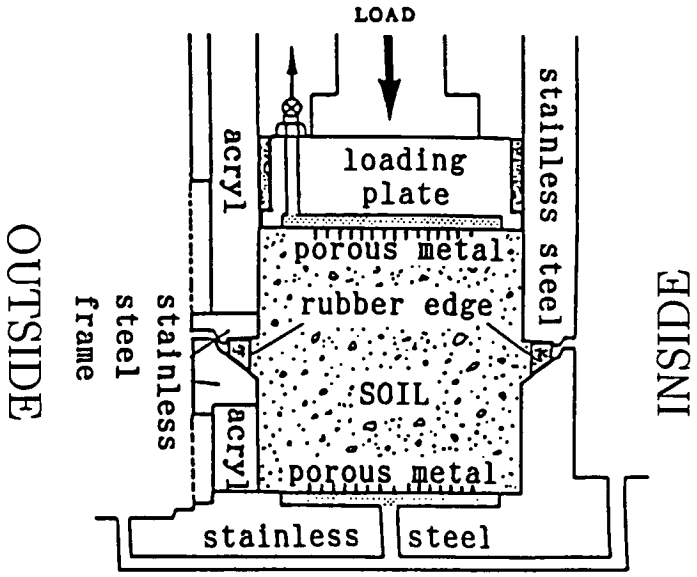

Fig. 5 Enlarged diagram of the annular sample box of the High-Speed High-Stress Ring Shear Apparatus.

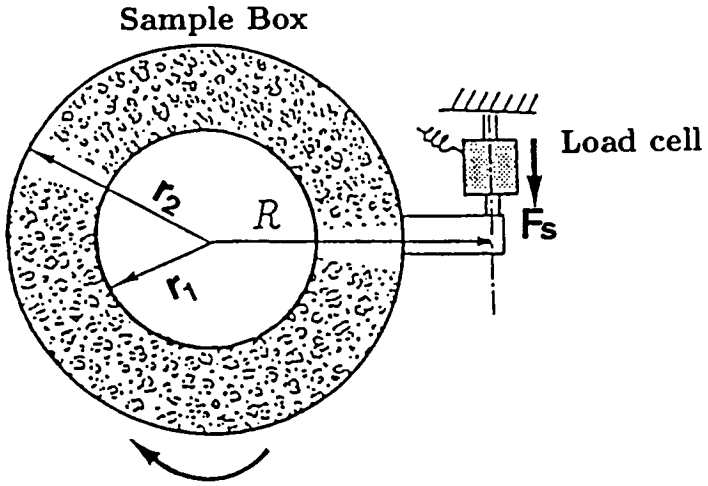

Fig. 6 Shear plane of the sample and the load cell for measurement of the shear resistance.

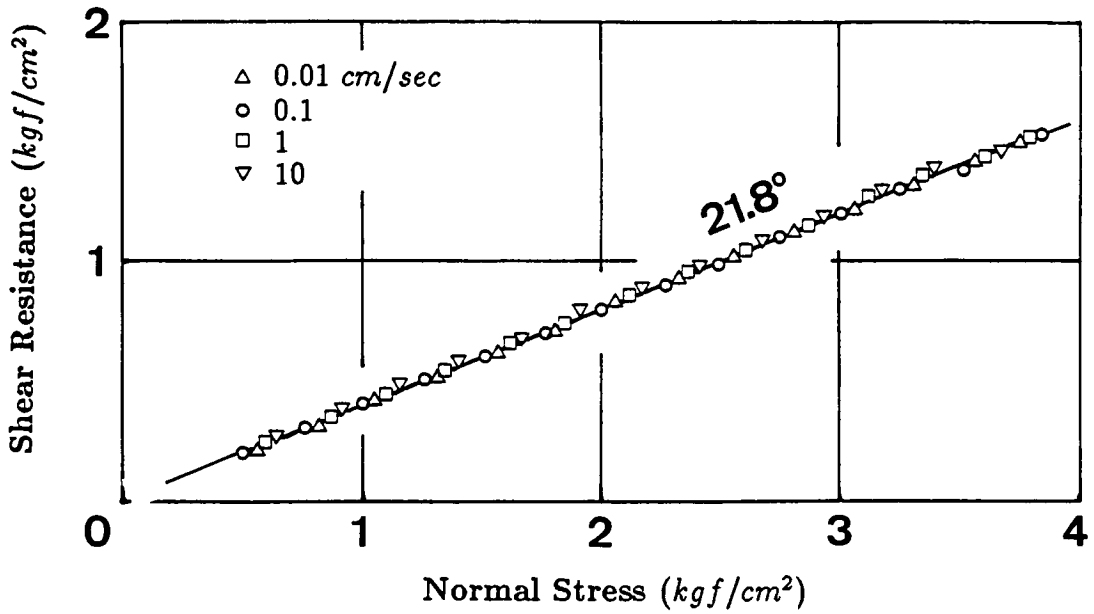

Fig. 7 Shear resistance of the dry 2mm glass beads in the Test Series A. Void ratio during shear $e = 0.62 \sim 0.69$.

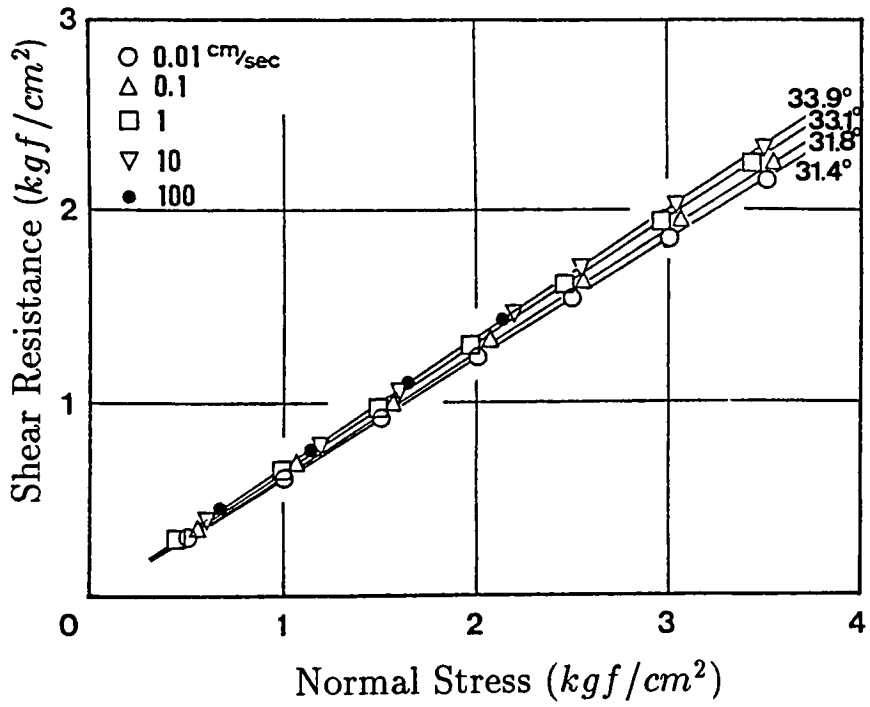

Fig. 8-1 Shear resistance of the dry Toyoura standard sands in the Test Series A. Void ratio during shear $e = 0.65 \sim 0.83$.

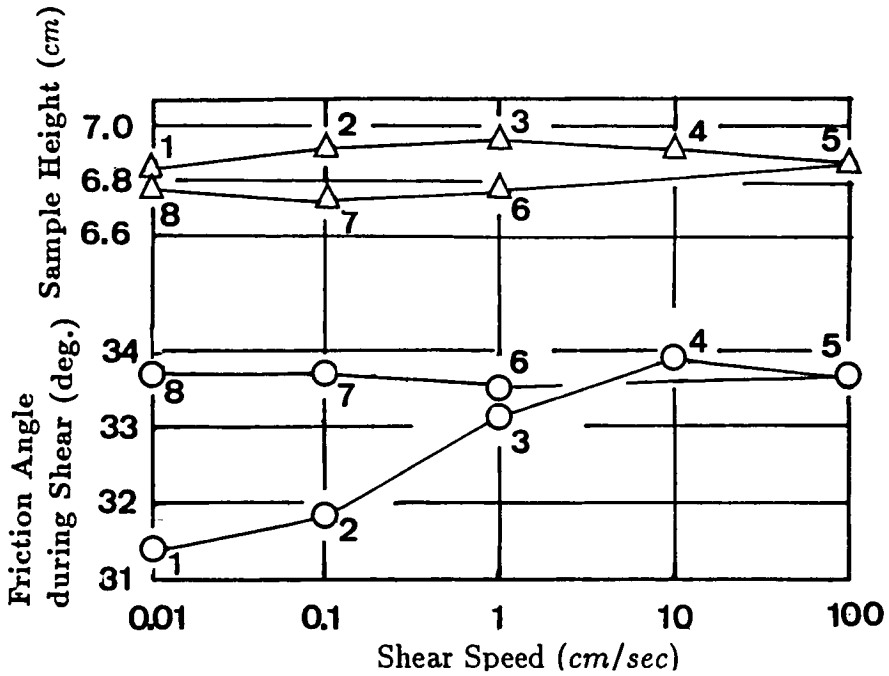

Fig. 8–2 Relation between the shear speed vs. the friction angle and final sample height of one cycle of shear test at each shear speed in the tests of **Fig. 8–1**.

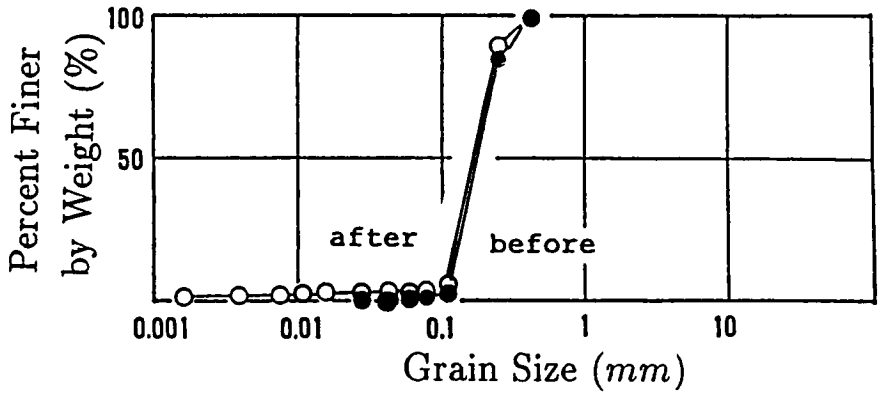

Fig. 8–3 Variation of the grain size distributions of the Toyoura standard sand sample before the test and the sample after the test of **Fig. 8–1**.

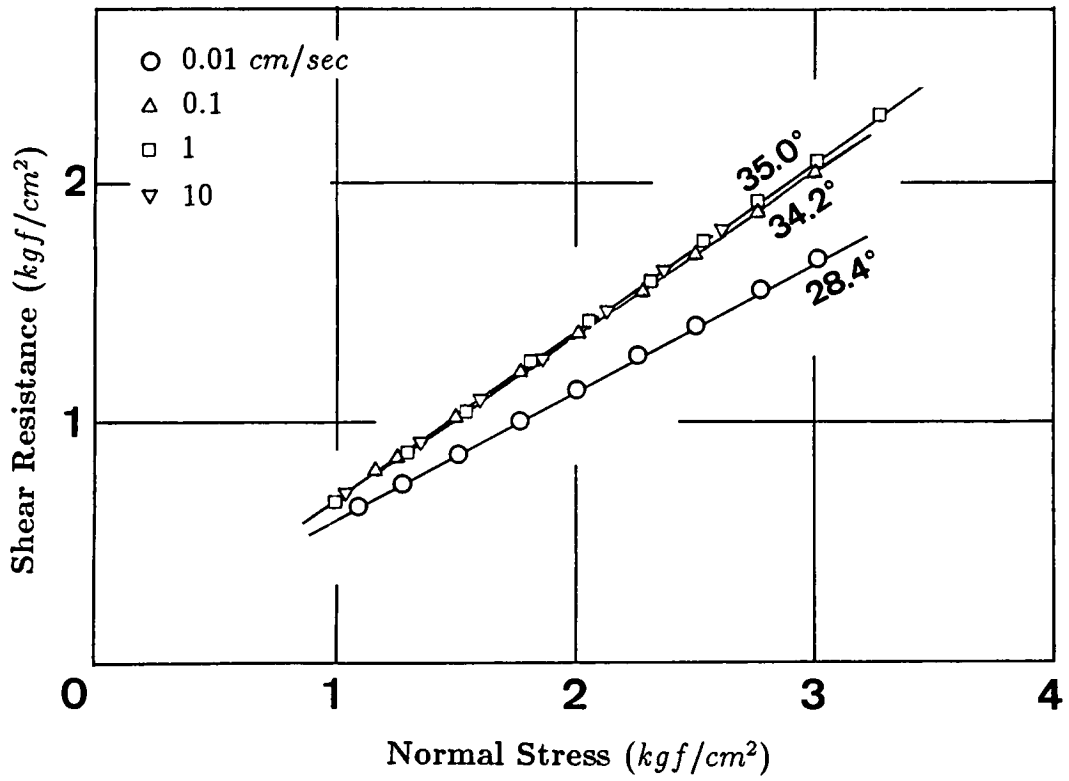

Fig. 9–1 Shear resistance of the dry bentonite clays in the Test Series A. Data on the process of reducing normal stress are plotted. Void ratio during shear $e = 1.74 \sim 2.04$.

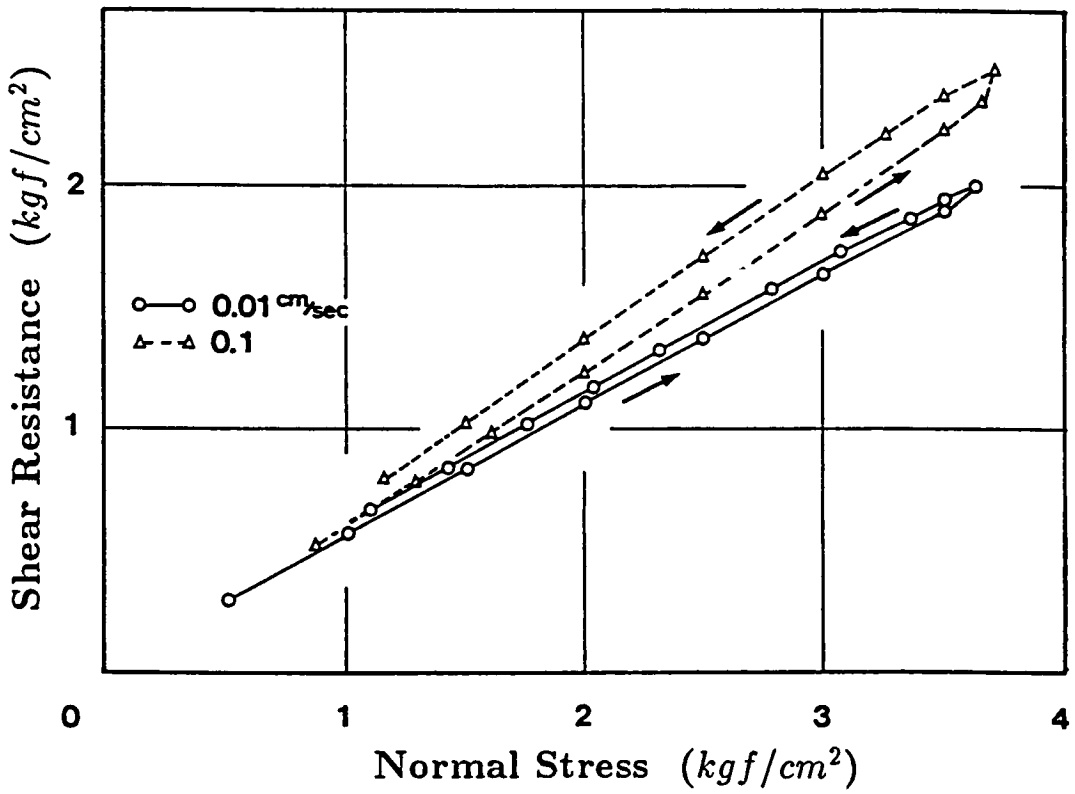

Fig. 9–2 Stress paths of the cycle of tests at 0.01 and $0.1cm/sec$ of **Fig. 9–1.** Void ratio during shear $e = 1.74 \sim 2.03$.

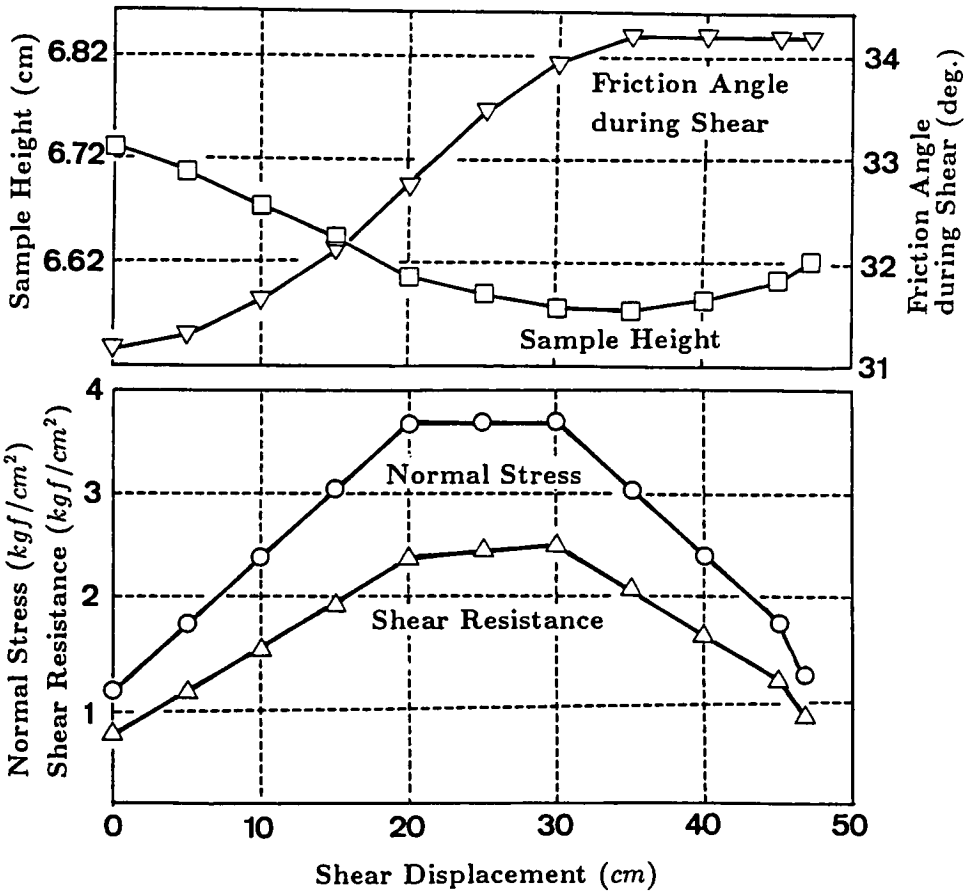

Fig. 9–3 Relation between shear displacement vs. normal stress, shear resistance, sample height and friction angle during shear in the test at $0.1cm/sec$ of **Fig. 9–2.**

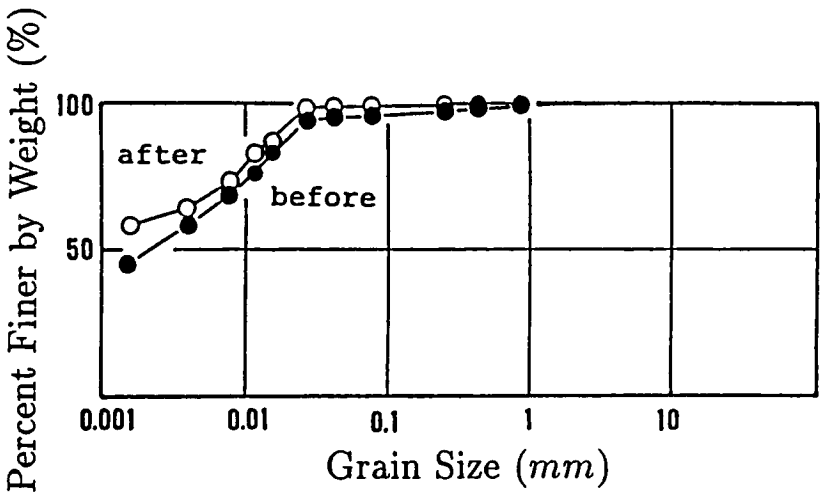

Fig. 9–4 Grain size distributions of the bentonite sample before the test and the sample from the shear zone after the test of Fig. 9–1.

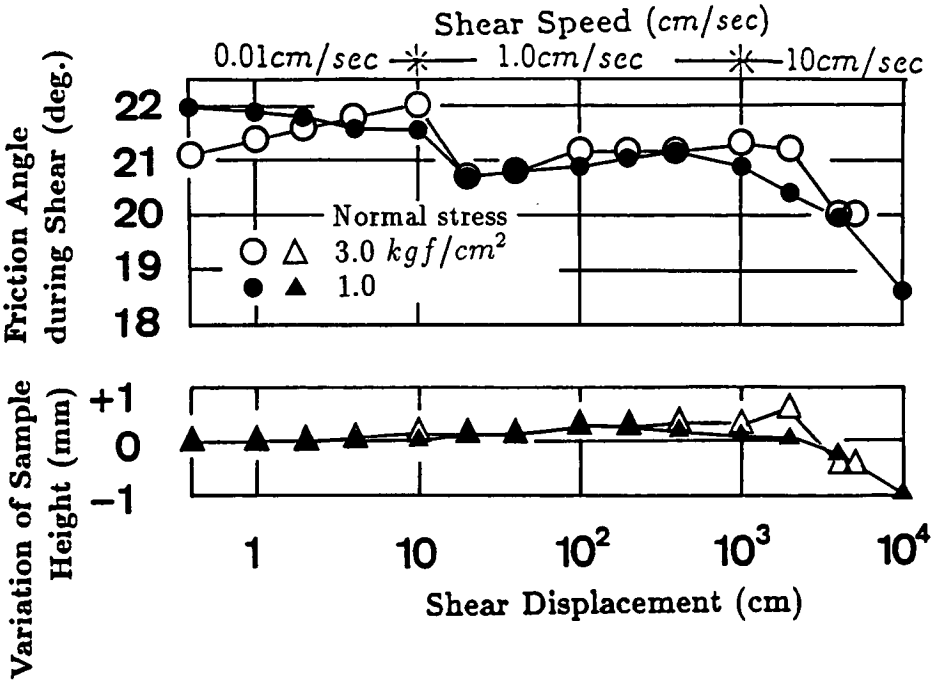

Fig. 10–1 Variation of the friction angle during shear and the sample height in the Test Series B on the 2mm glass beads.
The friction angle during shear decreased at the beginning of shear speed of 1cm/sec, probably due to gear change. It should be noticed that both of the sample height and the friction angle decreased beyond 10^3cm shear displacement.

Void ratio during shear is ;

$\sigma = 1.0 kgf/cm^2, e = 0.66 \sim 0.69.$

$\sigma = 3.0 kgf/cm^2, e = 0.63 \sim 0.64.$

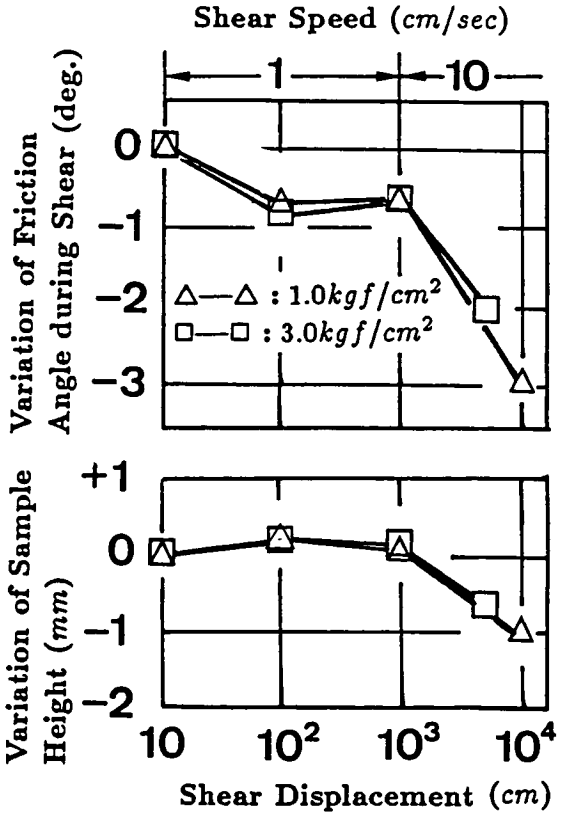

Fig. 10–2 Variation of the friction angle during shear and the sample height in the Test Series B on $2mm$ glass beads.
Data of **Fig. 11–1** are also plotted as rectangles. Each plot is the variation from the value at shear displacement $L = 10cm$.
Void ratio during shear is ;

$\sigma = 1.0kgf/cm^2, e = 0.66 \sim 0.69$

$\sigma = 3.0kgf/cm^2, e = 0.63 \sim 0.64$

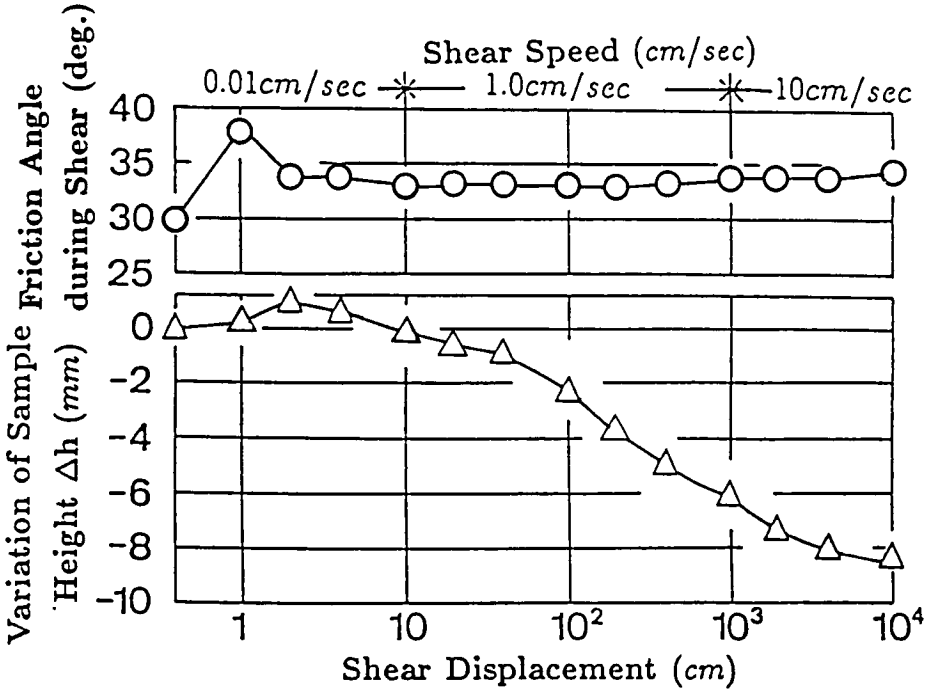

Fig. 11–1 Variation of the friction angle during shear and the sample height in the Test Series B on the Shirakawa river sand (grain size $=0.84 \sim 9.52mm$).
Normal stress $\sigma = 3.0kgf/cm^2$ Void ratio during shear $e = 0.56 \sim 0.76$.

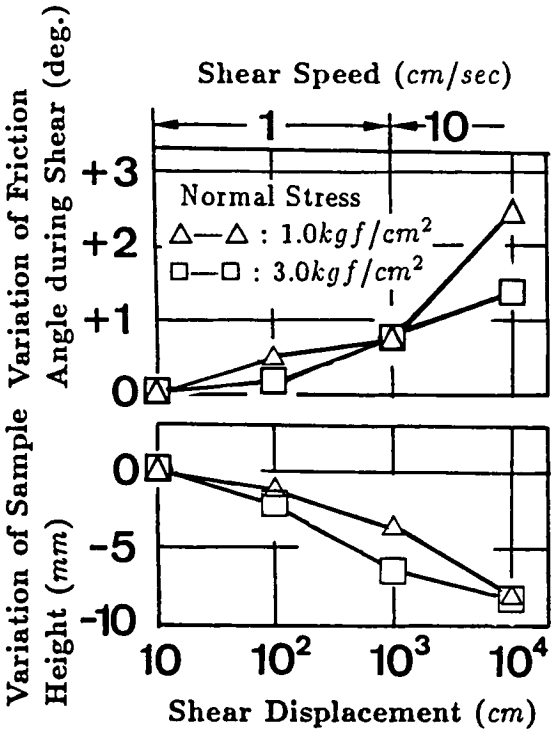

Fig. 11–2 Variation of the friction angle during shear and the sample height in the Tests Series B on the Shirakawa river sand.
Data of Fig. 11–1 are also plotted as rectangles. Each plot is the variation from the value at shear displacement $L = 10cm$.
Void ratio during shear is ;

$\sigma = 1.0kgf/cm^2, e = 0.61 \sim 0.80.$

$\sigma = 3.0kgf/cm^2, e = 0.56 \sim 0.76.$

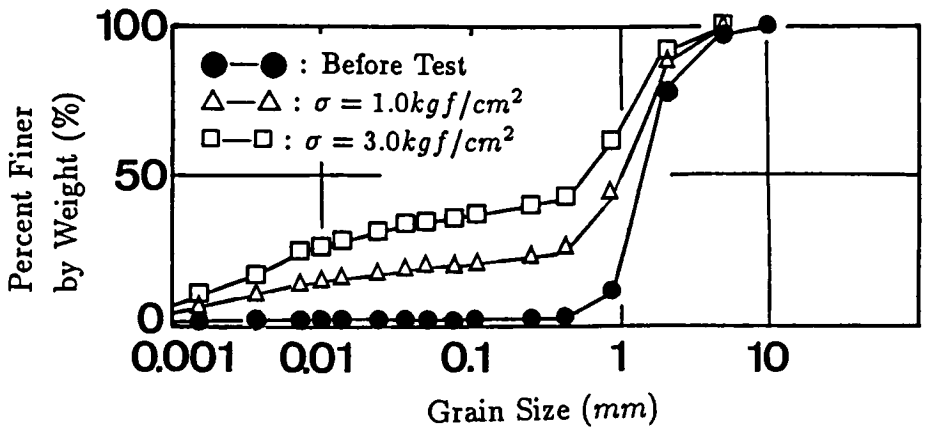

Fig. 11–3 Grain size distributions of the Shirakawa river sands sample before the tests and the samples taken from the shear zone after each test of **Fig. 11–2** under different normal stresses.

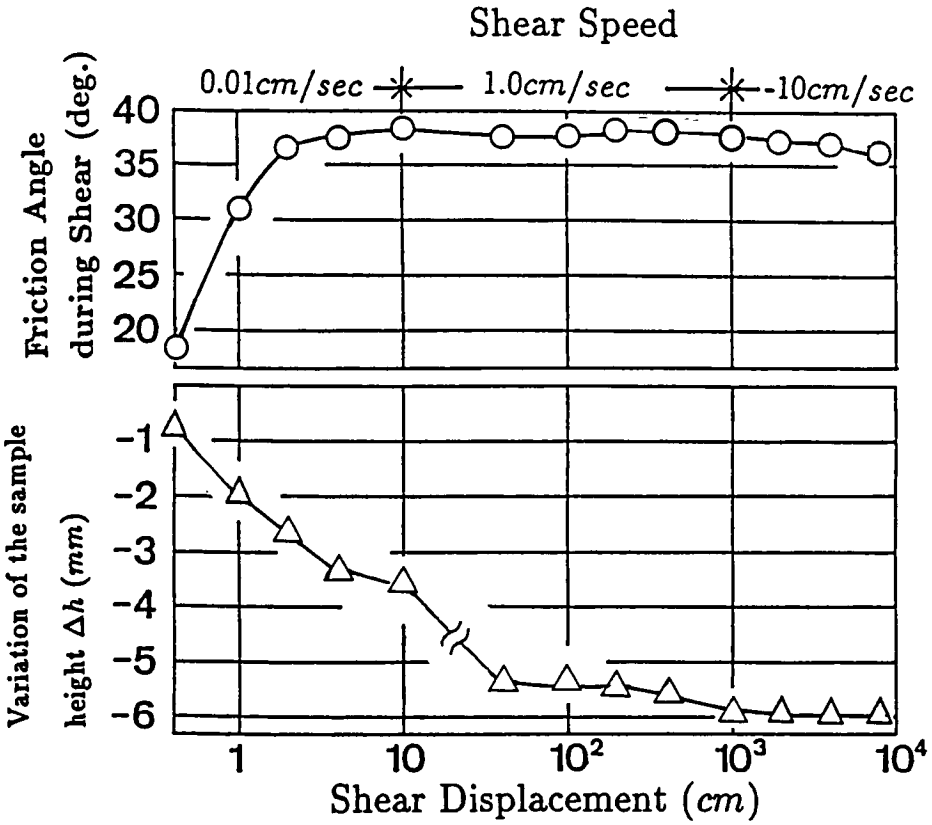

Fig. 12–1 Variation of the friction angle during shear and the sample height in the Test Series B on the Zentoku landslide soils (grain size $< 9.52mm$).
Because of a trouble in the measurement of sample height in changing the shear speed from 0.01cm/sec to 1cm/sec, measurement of the sample height was interrupted. It is indicated as the mark (⊣⊢).

Normal stress $\sigma = 3.0kgf/cm^2$. Void ratio during shear $e = 0.68 \sim 0.94$.

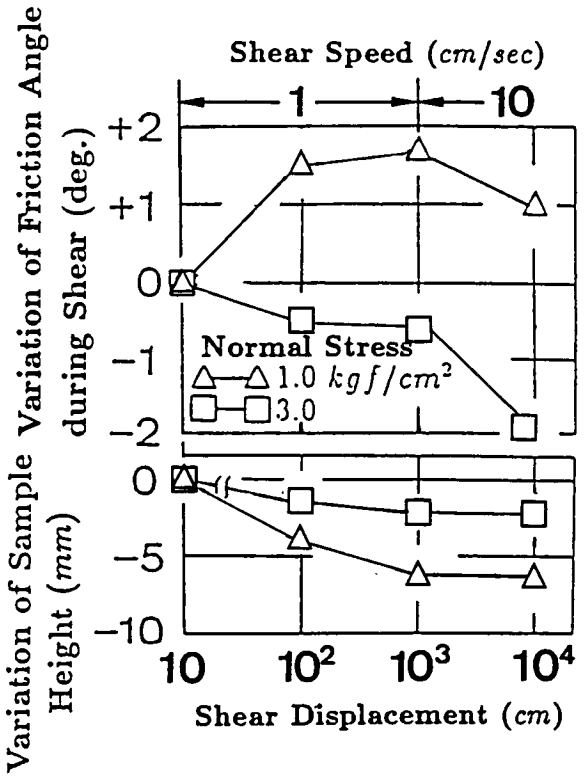

Fig. 12–2 Variation of the friction angle during shear and the sample height in the Tests Series B on the Zentoku landslide soils. Data of the test in **Fig. 12–1** are also plotted as rectangles. Each plot is the variation from the value at shear displacement $L = 10cm$.
Void ratio during shear is ;

$\sigma = 1.0kgf/cm^2, e = 0.68 \sim 0.96$

$\sigma = 3.0kgf/cm^2, e = 0.68 \sim 0.94$

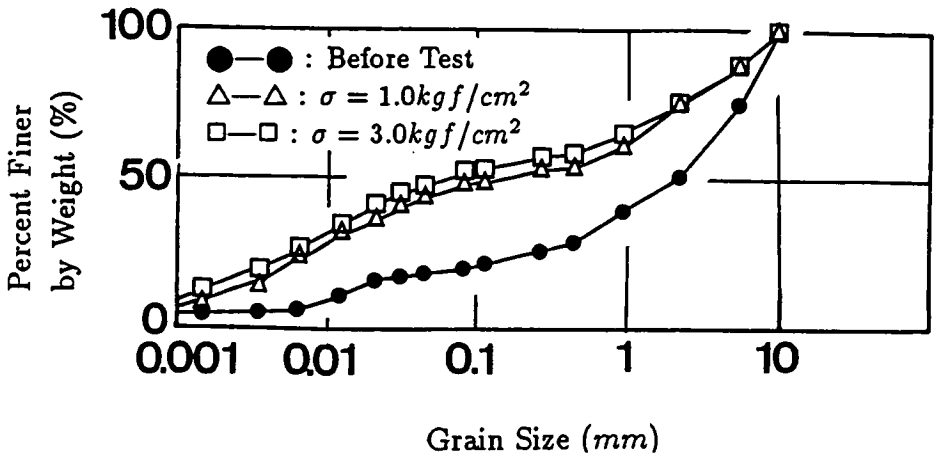

Fig. 12–3 Grain size distribution of the Zentoku landslide soil samples before the tests and the samples from the shear zone after each test of **Fig. 12–2** under different normal stresses.

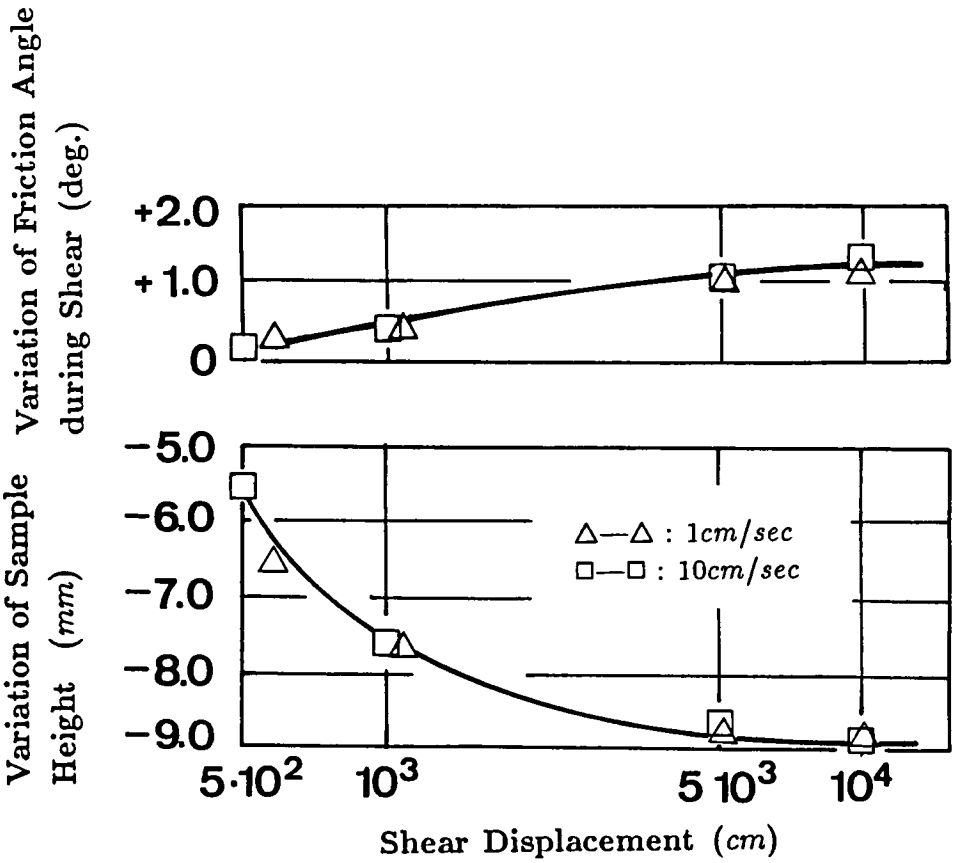

Fig. 13 Variation of the friction angle during shear and variation of the sample height in the tests on the Shirakawa river sand in the procedure shown in **Table 3.** The normal stress is $\sigma = 3.0 kgf/cm^2$.
This test is aimed at to examine the effect of shear speed history on the friction angle during shear in comparison with Test Series B (**Fig. 11–1**).

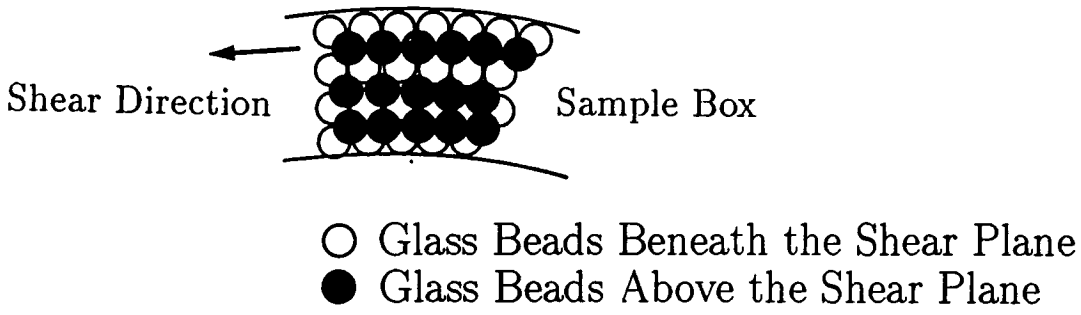

Fig. 14 Illustration of alignment of glass beads along concentric paths during shearing in the sample box of the ring shear apparatus.

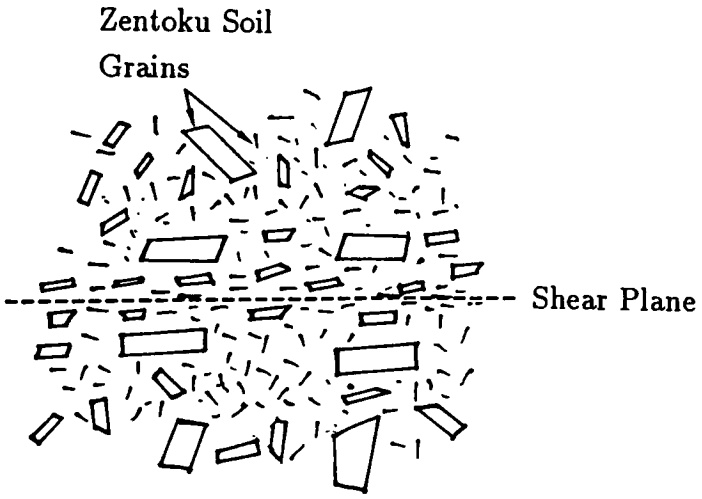

Fig. 15 Illustration of re-orientation of slender grains of the Zentoku landslide sample in the vicinity of the shear plane in the ring shear apparatus. This is drawn in the similar way with the illustration of re-orientation of clays during shear[23], in which the platy clay grains are replaced by slender crystalline-schist grains.

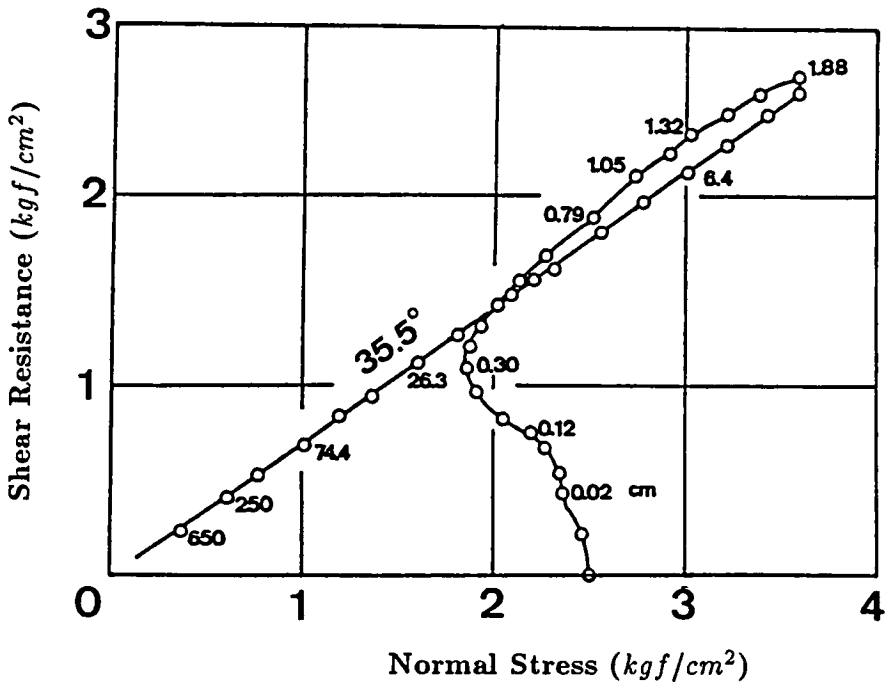

Fig. 16 Stress path of a ring shear test on the dry torrent deposits of the Denjo river in a constant volume condition (Fukuoka et al.[24]).
Void ratio during shear $e = 0.61$. Numerical values in the graph indicate the shear displacement.

Table 1. Parameters of previous ring shear tests.

Researcher	r_1 (cm)	r_2 (cm)	h (cm)	σ_{min} (kgf/cm^2)	σ_{max} (kgf/cm^2)	v_{min} (cm/sec)	v_{max} (cm/sec)	Samples	Rate effect
Novosad (1964)	3.2	6.3	2.9	0.0087	0.0247	0.48	47.5	coarse sands fine sands sugar 2.5mm glass beads	none
Scarlett & Todd (1969)	2.6	10.1	4.0	0.0216	0.0648	7.99	32.4	sands	none
Bridgwater (1972)	10.2	13.3	2.7	0.0064	0.255	18	192	2mm glass beads celon chips polypropylene chips polyethylene chips polyester chips	$+1.4°$ slight $+\Delta\tau$ slight $+\Delta\tau$ $+1.2°, +2.1°$ $-1.0°$
Hungr & Morgenstern (1984)	11.0	15.0	2.0	0.12	2.04	0.03	98	coarse sand sands and rock flour sands (saturated) polystylene beads	none none none none
Sassa et al. (1984)	15.0	24.0	9.0	0.04	0.40	0.01	90	1mm glass beads 0.2mm glass beads torrent deposits river sands	none none none none
Vibert et al. (1989) Fukuoka et al. (1990)	10.5	16.5	6.0	0.10	3.76	0.01	100	1mm glass beads torrent deposits Jizukiyama soils	$-2.0°$ $+1.5°$ $+3.7°$

r_1, r_2: inner and outer radius of annular sample box, h: sample height, $\sigma_{min}, \sigma_{max}$: min. and max. normal stresses, v_{min}, v_{max}: min. and max. shear speeds at the center of the sample box.

Table 2–1 Characteristics of samples for the Test Series A.

Sample	Diameter	Uniformity Coefficient	Shape	Crushability
Glass beads	$2mm$	1.0	round	uncrushable
Toyoura beach sands	$D_{50} = 0.2mm$	1.62	less angular	less crushable
Bentonite clays	$D_{50} = 0.003mm$	—	platy	crushable

Table 2–2 Characteristics of samples for the Test Series B.

Sample	Diameter	Uniformity Coefficient	Shape	Crushability
Glass Beads	$2mm$	1.0	Round	uncrushable
Shirakawa river sands (granite)	$D_{50} = 1.4mm$	1.89	less angular	crushable
Zentoku landslide soils (crystalline-schist)	$D_{50} = 2.0mm$	276	long & slender	crushable

Table 3 Test procedure of **Fig. 13**.

Shear Speed	Shear Displacement (m)
10cm/sec	0 – 5.0 5.5 – 10.0 10.5 – 50.0 50.5 – 100.0
1cm/sec	5.0 – 5.5 10.0 – 10.5 50.0 – 50.5 100.0 – 100.5

Photo. 1 The Ontake landslide in Japan, 1984.

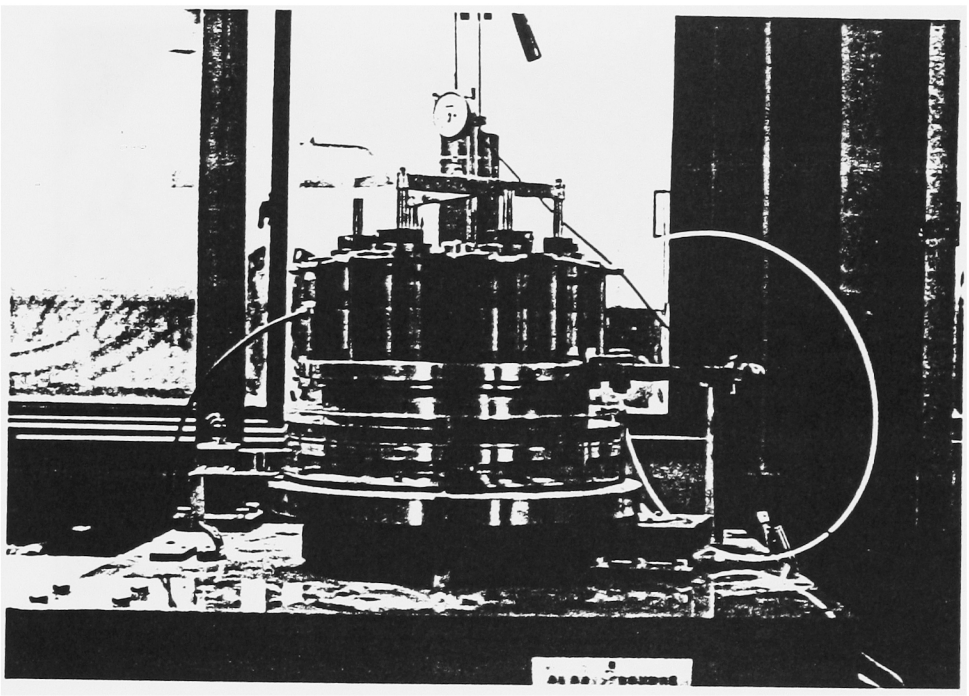

Photo. 2 Front view of the High-Speed High-Stress Ring Shear Apparatus.

Photo. 3 Shear plane of a bentonite sample after the test of **Fig. 9–1**.

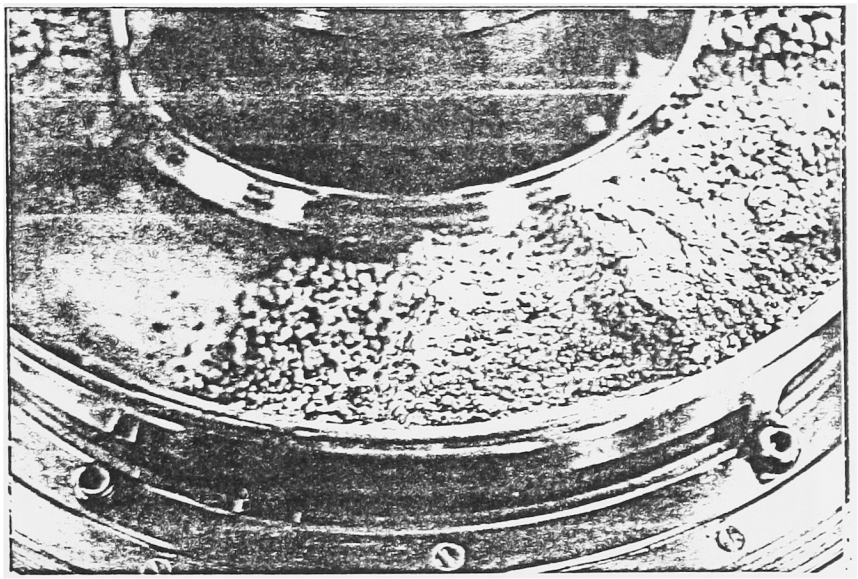

Photo. 4–1 Shear plane of the Shirakawa river sands after the test of **Fig. 11–1**. Fine ground sands were observed on the shear plane (at center).

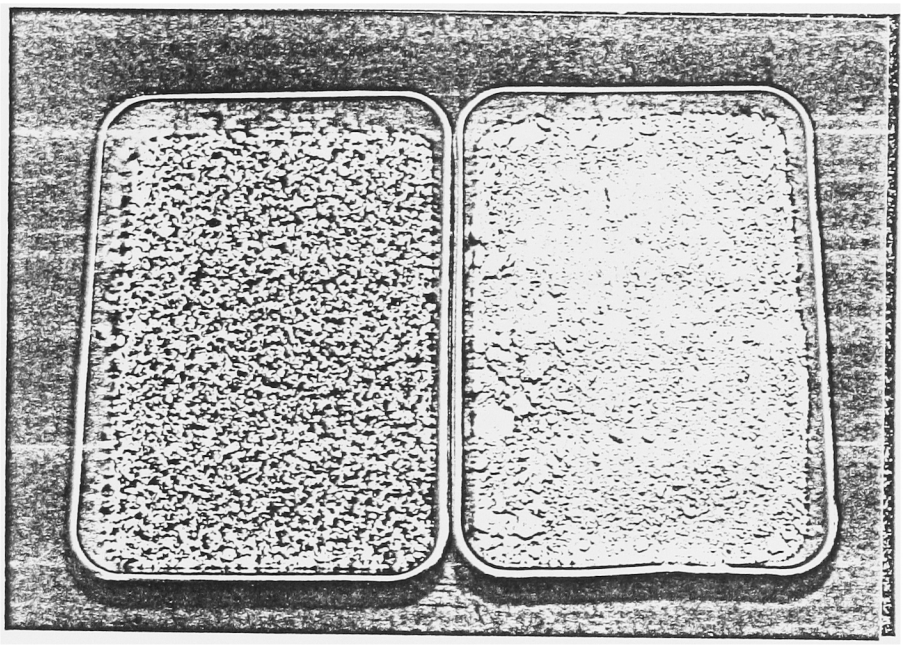

Photo. 4–2 Comparison of the Shirakawa River sand samples between before (on the left) and after (right) the test of **Fig. 11–1**.

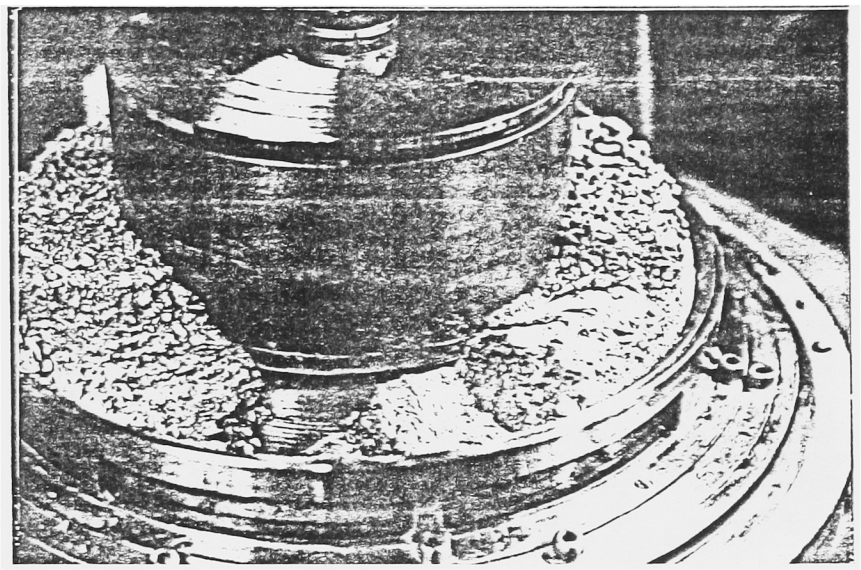

Photo. 5–1 Shear plane of the Zentoku landslide soils after the test of **Fig. 12–1**.

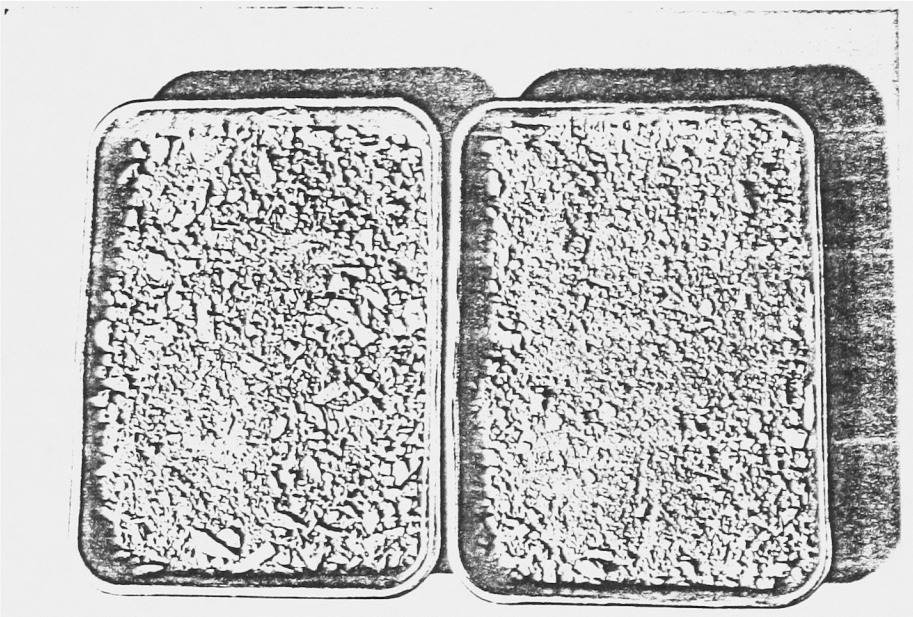

Photo. 5–2 Comparison of the Zentoku landslide soil sample between before (on the left) and after (right) the test of Fig. 12–1.